Anamet *Materials Engineering & Laboratory Testing*
26102 EDEN LANDING ROAD, SUITE 3 • HAYWARD, CALIFORNIA 94545 • (510) 887-8811 • FAX (510) 887-8427

Report No. 5005.7350 **May 8, 2020**

METALLURGICAL EVALUATION OF A RUPTURED DEPROPANIZER ACCUMULATOR DISCHARGE LINE INVOLVED IN THE JUNE 21, 2019 LOSS OF CONTAINMENT AND FIRE AT PHILIDEPHIA ENERGY SOLUTIONS REFINERY IN PHILIDELPHIA PENNSYLVANIA

Customer Authorization: CSB-1I25-19-0023

Report To: U.S Chemical Safety and Hazard Investigation Board
Attn: William Hougland
1750 Pennsylvania Ave. NW, Suite 910
Washington, DC 20006

1.0 INTRODUCTION

Metallurgical evaluation was performed on samples of ruptured 8-inch carbon steel depropanizer reflux line involved in the June 21, 2019 loss of containment, fire, and explosions at the Girard Point hydrofluoric acid alkylation unit in the Philadelphia Energy Solutions Refining and Marketing LLC (PES) Refinery, in Philadelphia, Pennsylvania. The metallurgical evaluation was performed at Anamet in Hayward, California, with participation by the U.S. Chemical safety Board (CSB) and representatives of other parties in this matter. The CSB reported the following background information. Post incident investigation found a ruptured carbon steel elbow in the subject line between V-11, the depropanizer accumulator, and T-6, the depropanizer distillation column. The ruptured elbow was on the discharge line of a pump that was not operating at the time of the incident. In addition, the ruptured elbow had separated from a horizontal run of the carbon steel line. A model of the depropanizer line in relationship to T-6 and V-11 is shown along with a post incident photograph of the ruptured elbow is shown in Figure 1. At the time of the event, the uninsulated subject line was operating at a pressure of about 380 psig and a temperature of about 100 °F. The approximate composition of process fluid in the piping was 94.7-wt% propane, 2.8-wt% additional hydrocarbons, and 2.5-wt% hydrofluoric acid. The ruptured ASTM A 234 carbon steel elbow was believed to have been part of the original alkylation unit construction, circa 1973.

1.1 Summary of Findings

Based on the results of this evaluation, rupture of the subject T1 elbow by internal pressure resulted from extensive uniform corrosion that reduced the wall thickness to as little as 0.011-inch. Fracture of the T1 elbow from the T4 pipe occurred after the elbow rupture and initial release of hydrocarbons, and was likely the result of subsequent fire and explosions. Accelerated corrosion of the ruptured elbow T1 conformed to industry experience with carbon steel components that contain elevated levels of the residual elements nickel and copper as described in API 571 and API 751. The chemical composition of the ruptured elbow T1 met the chemical composition requirements of ASTM A 234 in 1965, but did not meet the requirements of the 2015 version of

the standard or the guidelines regarding residual elements in API 571 because the nickel and copper concentrations were greater than allowed. The elbow T2 and the pipe sections T3 and T4 met the chemical composition requirements of the current versions of ASTM A234, and ASTM A106 in addition to the guidelines on residual elements in API 571.

2.0 EVALUATION

2.1 Visual Examination

By agreement with all parties, the subject samples were shipped to Anamet without cleaning. Although it is common practice to clean samples and equipment from alkylation units prior to release from a refinery, particularly with hydrofluoric acid (HF) alkylation units, in this case all parties agreed that the combination of fire suppression water and HF mitigation applied to the site during and after the incident rendered the samples safe to transport with appropriate labels indicating potential hazards. Upon receipt at Anamet, pH indicators were used to survey the samples for low pH. No low pH and, therefore, no indications of the presence of acid was detected.

The samples were received as two separate pieces of evidence, E004 and E012. The E004 evidence consisted of the ruptured elbow identified as T1, welded to another elbow identified as T2, welded to a section of pipe identified as T3. The end of T3 opposite the elbows had been cut to allow removal from the incident site. Sample E012 consisted of a section of pipe referred to as T4, one end of which had fractured from the ruptured elbow T1. The fractured end of T4 was out-of-round with a similar shape to that of the fractured end of T1. The end of T4 opposite the fracture had been cut to allow removal from the incident site. A photograph of the subject piping prior to removal from the site is shown in Figure 1a, and photographs of the samples after receipt are shown in Figure 2 through Figure 5. Prior to the metallurgical evaluation, a three dimensional model of E004 was captured by laser scanning, which requires small light reflectors attached to the part being scanned. The magnet backed reflectors appear as spots in the photographs. Results of the laser scanning were not relied on for the metallurgical evaluation, but the results were made available to all parties in this matter.

Rupture of elbow T1 occurred on the outside of the bend. Based on the shape of the rupture, failure initiated near the location indicated in Figure 2. The rupture path from the origin was approximately parallel to the longitudinal axis of the elbow, which indicates that failure was driven by hoop stresses developed from internal pressure. A flap formed by the rupture was displaced to the outside of the uninsulated line, also indicative of rupture driven by internal pressure. The remaining wall thickness near the rupture origin was as low as 0.023-inch, measured by point anvil micrometer without cleaning tenacious scale from the region. Thickness measurements along the edges of the rupture and rupture flap averaged 0.056-inch and did not exceed 0.120-inch. The locations of thickness measurements are shown in Figure 6 and the corresponding results are listed in Table 1. Visual examination indicated this range of thickness was consistent across the majority of the outside bend in the elbow. A V-shaped side crack that intersected the rupture origin and propagated transverse to the longitudinal axis was predominantly driven by events secondary to the rupture initiation and release of hydrocarbons.

Examination of the T1 elbow to T4 pipe fracture indicated that fracture occurred through the elbow base metal. Thickness measurements taken around the circumference of T1 had an average value of 0.151-inch. Thickness measurements of the T4 pipe wall adjacent to the weld toe had an average

value of 0.287-inch, and the wall thickness at the cut end had an average thickness of 0.302-inch. The locations of thickness measurements around the fractured end of T1, the cut end of T3,and both ends of T4 are shown in Figure 6b, Figure 4, Figure 5b, and Figure 5c, respectively. Corresponding thickness values are listed in Table 2 through Table 4. The macroscopic morphology of the fracture along the top edges of T1 and T4 indicated global shear loading consistent with the post incident position of T1 lower than T4, as shown in Figure 1b. Because the T1 to T4 fracture would have released pressure within T1 and the T1 rupture was driven by internal pressure, the T1 rupture must have preceded the fracture between T1 and T4.

Transverse cuts were made to separate elbow T1 from elbow T2, and elbow T2 from pipe T3, indicated by dashed lines in Figure 3a. The elbows were also cut along their longitudinal plane of symmetry. The longitudinal sections demonstrated a large difference in wall thickness between elbow T1 and elbow T2. Photographs of one half of T1 and one half of T2 are shown in Figure 7 and Figure 8, respectively. Wall thickness measurement results are listed in Table 5 and Table 6.

A thick, flakey, rust scale was present on the outside surfaces of the samples, consistent with exposure to fire suppression water. Immediately inside the fractured ends of T1 and T4, the scale was thin and mostly tenacious. Within T1, the inside scale transitioned to friable rust that was thicker below a water level line, indicated in Figure 7. Standing water within T1 is visible in Figure 1b. Accumulation of rust was greatest within elbow T2. At the cut end of pipe T3, some longitudinal bands of the inside surface scale were dark colored and tenacious under a light rust bloom. Other longitudinal bands of the dark scale in T3 were partially lifted from the surface and mixed with rust. Both inside scale morphologies are visible in Figure 4, at the cut end of T3. Similar internal scale morphologies were present in the pipe sample T4, as shown in Figure 5.

Identification stamps were present on the outside surface of elbows T1 and T2, but were difficult to read through the scale. Scale on the stamped regions was removed by scrubbing with a silicon carbide abrasive pad and water. Photographs of the stamps after scrubbing are shown in Figure 9 and Figure 10. Elbow T1 was stamped: MADE IN USA 8 STD B&W WPB 1LDM, where 8 STD indicates 8-inch nominal pipe size standard Schedule; B&W is the manufacturer's identification; WPB indicates the seamless fitting steel Grade, and 1LDM should be a heat or lot code. These stamps partially overlapped a lighter set of stamps that followed the same general sequence of: 8 STD followed by a mostly illegible manufacturer's identification, partially legible grade designation, and heat or lot code DFH1Y. The CSB suggested that the partially legible grade designation was YOLOY, an older trade name for 2-wt% nickel, 1-wt% copper, 0.25-wt% carbon steel marketed for atmospheric corrosion resistance.[1] Chemical analysis, described in Section 2.2, found that the composition of the T1 elbow was consistent with Yoloy steel. In contrast, only one set of stamps was present on elbow T2, which read MADE IN USA 8 STD B&W WPB 1LDM.

2.2 Chemical analysis

Quantitative chemical analysis by spark optical emission spectroscopy and LECO combustion was performed on samples of T1, T2, T3, T4, and the welds that joined T1 to T2, T2 to T3, and T1 to T4. Chemical analysis results are listed in Table 7 through Table 9. For initial construction in 1973, ASTM A 234-65 was the active specification for the elbows, and states that Grade WPB

[1] SYMPOSIUM ON HIGH-STRENGTH CONSTRUCTIONAL METALS, AMERICAN SOCIETY FOR TESTING MATERIALS, March 4, 1936, P. 13.

fittings shall meet the chemical composition requirements of ASTM A 106 carbon steel pipe.[2] Therefore, ASTM A 106-68 chemical composition requirements are also listed along with the analysis results. The elbow and pipe samples met the chemical composition requirements in effect at the time of original construction. However, elbow T1 only met the stated requirements because the elements nickel and copper were not controlled for these product forms and service circa 1973. The chemical composition of T1 was consistent with Yoloy steels. Requirements for Yoloy steel are also listed in Table 7. Steels with composition similar to Yoloy were developed for atmospheric corrosion resistance, often referred to as weathering steels, and are now classified as high-strength low-alloy steels

Year 2015 versions of the standards, ASTM A234-15 and A106-15, control more elements than the 1965 and 1968 versions of the standards. The year 2015 standards also contain supplementary requirements that may be agreed upon between the buyer and seller. In the A106-15 standard, Supplementary Requirement S9 is specifically written for carbon steel pipe in HF alkylation service because of a correlation between elevated levels of residual elements and accelerated corrosion of carbon steel in environments that contain HF.[3][4] Residual elements (RE) are elements commonly found in an alloy but not intentionally added.[5] In carbon steels, RE include chromium, copper, and nickel. The ruptured elbow T1 would have failed the chemical composition requirements of A234-15 and A106-15, listed in Table 10, because the nickel and copper concentrations exceeded the maximum allowable.

In addition to control of RE current versions of A234 and A106 also place limits on the carbon equivalent (CE). The maximum attainable hardness of carbon steels is most strongly affected by the carbon concentration. However, other elements also affect the hardness, and the CE is used to account for the influence of elements other than carbon. The relationship for carbon equivalent referenced in A234-15 and A106-15 is:

$$CE = C + Mn/6 + (Cr+Mo+V)/5 + (Ni+Cu)/15$$

The CE results for the elbows, pipe, and weld metal are listed in Table 7 trough Table 9. All of the samples met the stated carbon equivalent requirements.

Chemical analysis was performed by energy dispersive x-ray spectroscopy[6] (EDS) and x-ray diffraction on specimens of internal scale scraped from the samples. The two techniques are complimentary in that EDS detects the presence of elements and XRD analyzes crystallographic structure. Collection of the samples was performed early in the visual examination phase of this work. The locations from which the specimens were scraped are listed in Table 11, along with a summary of the EDS and XRD results. Although x-ray Kα peaks from fluorine and Lα peaks

[2] ASTM A 234-65, Standard Specification for FACTORY MADE WROUGHT CARBON STEEL AND FERRITIC ALLOY STEEL WELDING FITTINGS, ADOPTED 1964, REVISED 1965.
[3] API RP 751 Safe Operation of Hydrofluoric Acid Alkylation Units
[4] API RP 571 Damage Mechanisms Affecting Fixed Equipment in the Refining Industry
[5] Metals Handbook, 6th Edition, Vol. 1, Properties and Selection of Metals, American Society for Metals, Metals Park Ohio, p 31, 1961,
[6] The EDS analysis method used here detects the presence of elements from boron (B) to uranium (U), atomic numbers from 5 to 92 in the periodic table. EDS data alone are, however, insufficient to differentiate chemical compounds such as oxides, hydroxides, or carbonates or to characterize organic materials that consist of carbon (C), hydrogen (H), and nitrogen (N) only.

from iron overlap, comparison of the ratios of iron peak amplitudes and modeled spectra provided confidence that fluorine (F) was detected by EDS in all of the specimens. Intense peaks from iron (Fe), and lower amplitude peaks from elements such as chromium (Cr), nickel (Ni), copper (Cu), and silicon (Si) commonly found in carbon steel corrosion product were detected. Calcium (Ca) and magnesium (Mg) were also detected. The presence of fluorine in the scale is consistent with HF corrosion of carbon steel. Representative EDS spectra are shown in Figure 11.

Specimens of scale that represented the range of sampled locations were analyzed by x-ray diffraction, subcontracted to EAG Laboratories in Sunnyvale, CA. Iron fluoride compounds were found to comprise a large percentage of the scale that was sampled from the cut ends of T3 and T4. Iron fluorides were not detected in specimens sampled from near the rupture and fracture between T1 and T4, likely the result of scale loss through thermal expansion and subsequent spallation or ablation of the scale during the fire.

2.3 Metallography

Longitudinal sections were prepared through each of the three welds, through the rupture origin on the flap, and through base metal of T1, T2, T3, and T4 unaffected by the welds, as indicated by dashed lines in Figure 6a and Figure 12. All sections, T1 was much thinner than the other samples, and the weld heat affected zone (HAZ) of T1 and T2 were thinner than the unaffected base metals. Photographs of the weld and flap sections along with representative micrographs are shown in Figure 13 through Figure 25. The microstructure of elbows T1 and T2 consisted of bands of spheroidized carbide in ferrite. In the flap section, the grain size was less than that in T1 base metal sections, indicative of recrystallization from the heat of the fire. The microstructure of pipe T3 and T4 consisted of fine pearlite and ferrite. No unusual microstructures for carbon or high-strength low-alloy steels were revealed by metallography.

2.4 Mechanical Testing

Knoop 500-gram load hardness testing was performed in accordance with ASTM E378-17 on the base metal sections unaffected by welding and on the weld sections prepared for metallography.[7] Results were converted to Brinell hardness according to ASTM E140-12. The average converted values of three indents in each of T1, T2, T3, and T4 were 235, 213, 166, and 191, respectively. Hardness indents on the weld sections were spaced approximately 0.050-inch apart in the weld metal and weld heat affected zone (HAZ). The results are listed in Table 12 through Table 14. The hardness of T1 was consistently greater than the hardness of T2, T3, and T4, a result of the greater concentration of nickel and copper in T1 compared to the other samples.

A number of converted hardness readings exceeded the maximum allowable hardness of 201 HB for Grade WPB in ASTM A234-65. However, no indications of particularly hard zones were detected, which is consistent with the carbon equivalent values calculated from chemical analysis results. Although it can be expected that the as-welded hardness was changed by the heat of the fire, all other evidence gathered indicates ductile fracture of the T1 HAZ and, therefore, no as-welded hard zones were present that would have caused brittle fracture.

Longitudinal tensile specimens were machined from the T3 pipe, centered on a region approximately 12-inches from the T3 to T2 weld. The specimens were tested in accordance with

[7] ASTM E370-17, Standard Test Method for Microindentation Hardness of Materials

ASTM A370-19 at ambient laboratory temperature.[8] Test results are listed in Table 15, along with the tensile requirements of ASTM A 106-68. The tensile strength and yield point of all three specimens exceeded the specified minimum requirements. The elongation of specimens 2 and 3 slightly exceeded the minimum requirement, but the elongation of specimen 1 was slightly less than the 30% minimum required by the standard.

Transverse Charpy V-notch impact test specimens were machined from the T3 pipe approximately 6-inches from the T3 to T2 weld and tested in accordance with ASTM A370-19 at ambient laboratory temperature.[7] The pipe wall thickness dictated subsize specimens according to the standard. The results are listed in Table 16. No impact test requirements are specified by ASTM A 106-68 or A106-15. However, the impact test results provide no indication for concern over the toughness of T3.

3.0 DISCUSSION

Most equipment in hydrofluoric acid alkylation units are constructed of carbon steel, which in general has proven to have sufficiently low corrosion rates.[9] Sufficiently low corrosion rates are rates that can be predicted and monitored reliably. Accelerated corrosion rates refer to rates that are faster than predicted or faster than can be safely monitored. Often, accelerated corrosion rates are relative to the majority of the system, referred to as preferential corrosion. Accelerated corrosion rates of particular components in HF alkylation units, such as the subject ruptured elbow T1, have been correlated with elevated levels of residual elements (RE) in carbon steels, in particular, nickel, copper, and chromium. Recommended limits on carbon and RE are given in API 571 as:[10]

Base metal $\%C > 0.18$ wt% and $\%Cu + \%Ni < 0.15$ wt%

Weld metal $\%Cu + \%Ni + \%Cr < 0.015$-wt%

As listed in Table 7, elbow T1 met the recommended carbon requirement but exceeded the recommended RE concentrations. The weld metals between T1 and T2 and T1 and T4 also failed to meet the RE requirement. However, none of the weld metals suffered accelerated corrosion as did the ruptured elbow T1. It is noted in API 571 that preferential corrosion may not always conform to prediction based on RE concentration.

Although the mechanism of accelerated corrosion in elevated RE carbon steels has not been agreed upon, formation of protective scale or film is essential to providing sufficiently low corrosion rates in all alloys. Therefore, disruption of protective scale is necessary to result in accelerated corrosion. Formation of iron fluoride scale is considered key to successful use of carbon steels in HF alkylation service. Consequently, the role of RE in carbon steel corrosion by HF must involve differences between scale formed by low RE steels and elevated RE steels. However, the details of the difference are not well established.

[8] ASTM A370-19, Standard Test Methods and Definitions for Mechanical Testing of Steel Products
[9] API Reccomended Practice 751, Safe Operation of Hydrofluoric Acid Alkylation Units, Fourth Edition, May 2013.
[10] API 571, Damage Mechanisms Affecting Fixed Equipment in the Refining Industry, Second Edition, April 2011, p.5-23.

Two sets of identification stamps had been made on the ruptured elbow T1. The first, lighter stamp indicated the elbow was Yoloy steel. The second, heavier stamp indicated the elbow was WPB steel. Yoloy was a trade name for a high-strength low-alloy steel to which copper and nickel were intentionally added to increase the atmospheric corrosion resistance and tensile yield strength.[11] In 1961, the Metals Handbook indicated:

> "As defined in in ASTM A242, high-strength low-alloy steel contains 0.22% C max and 1.25% Mn max, plus other alloying elements as will give the minimum yield point prescribed for various thicknesses. Also according to ASTM A242: it is intended that these alloying elements shall be such that the atmospheric corrosion resistance of this steel will be materially increased". [12]

In contrast, WPB was and still is a grade of carbon steel. In 1961, the Metals Handbook defined carbon steels:

> "Steel containing carbon up to about 2% and only residual quantities of other elements except those added for deoxidation, with silicon usually limited to 0.60% and manganese to about 1.65%."[13]

At the time the subject elbows were installed, the chemical composition requirements for WPB did not explicitly limit RE concentrations because, by definition, RE are not intentionally added and are present only in small concentrations. However, nickel and copper were intentionally added to Yoloy steel to increase tensile yield strength and atmospheric corrosion resistance compared to carbon steel. Consequently, Yoloy was classified as a high-strength low-alloy steel, and therefore, it was inaccurate to stamp the ruptured elbow as WPB, which is a carbon steel.

Carbon steel specifications and definitions have evolved to include RE limits. For example, recent versions of ASTM A234 have maximum limits on copper, nickel, chromium, and vanadium in addition to limits on the sum of those elements. These limits are irrespective of the intended service conditions. The need for increased control of RE in carbon steel is attributed in part to the increased use of scrap metal as opposed to steel smelted from iron ore alone.

[11] SYMPOSIUM ON HIGH-STRENGTH CONSTRUCTIONAL METALS, AMERICAN SOCIETY FOR TESTING MATERIALS, March 4, 1936, P. 13.
[12] Metals Handbook, 6th Edition, Vol. 1, Properties and Selection of Metals, American Society for Metals, Metals Park Ohio, p 87, 1961.
[13] Ibid., p 87.

4.0 CONCLUSIONS[14]

The following conclusions are based upon the submitted samples and the evidence gathered:

1. Rupture of the subject T1 elbow by internal pressure resulted from extensive general corrosion that reduced the wall thickness to as little as 0.011-inch.

2. Fracture of the T1 elbow from the T4 pipe occurred after the elbow rupture and initial release of hydrocarbons, and was likely the result of subsequent fire and explosions.

3. Accelerated corrosion of the ruptured elbow T1 conformed to industry experience with carbon steel components that contain elevated levels of the elements nickel and copper as described in API 571 and API 751.

4. Stamps on the ruptured elbow T1 accurately identified the subject as Yoloy, a high-strength low-alloy steel to which nickel and copper were intentionally added to provide increased yield strength and atmospheric corrosion resistance compared to carbon steel.

5. A second set of stamps on the ruptured elbow T1 incorrectly identified the subject as WPB, a grade of carbon steel.

6. The chemical composition of the ruptured elbow T1 met the chemical composition requirements of ASTM A 234, Grade WPB in 1965 because WPB requirements applied to carbon steel and, therefore, did not place limits on residual elements such as copper and nickel.

7. The chemical composition of the ruptured elbow T1 did not meet the requirements of the 2015 version of ASTM A234 for Grade WPB because the nickel and copper concentrations were greater than allowed.

8. The elbow T2 and the pipe sections T3 and T4 met the chemical composition requirements of the current versions of ASTM A234, and ASTM A106 in addition to the guidelines on residual elements in API 571.

Prepared by:

Sam McFadden, Ph. D.
Associate Director of Laboratories

[14] The conclusions in this report are based upon the available information and evidence provided by the client and gathered by Anamet, within the scope of work authorized by the client, and they are hereby presented by Anamet to a reasonable degree of engineering and scientific certainty. Anamet reserves the right to amend or supplement its conclusions or opinions presented in this report should additional data or information become available, or further work be approved by the client.

Table 1
Thickness Measurement Results for the Rupture Flap and Rupture Edge
From Locations Indicated in Figure 6a

Sample Region	Location Number	Wall Thickness (inch)
T1 Rupture Flap	1	0.120
	2	0.102
	3	0.091
	4	0.077
	5	0.059
	6	0.044
	7	0.040
	8	0.035
	9	0.041
	10	0.031
	11	0.027
	12	0.023
	13	0.025
	14	0.032
	15	0.031
	16	0.031
	17	0.029
	18	0.032
	19	0.041
	20	0.050
	21	0.067
	22	0.077
	23	0.086
	24	0.096

Sample Region	Location Number	Wall Thickness (inch)
T1 Rupture Edge	25	0.100
	26	0.088
	27	0.077
	28	0.064
	29	0.054
	30	0.050
	31	0.042
	32	0.045
	33	0.025
	34	0.023
	35	0.025
	36	0.025
	37	0.040
	38	0.037
	39	0.039
	40	0.044
	41	0.061
	42	0.074
	43	0.092
	44	0.113
	45	0.072
	46	0.091
	47	0.082
	48	0.056

Table 2
Thickness Measurement Results from the T1 Side of the T1 to T4 Fracture
From Locations Indicated in Figure 6b

Sample Region	Location Number	Wall Thickness (inch)
T1 Side of T1-T4 Fracture	49	0.167
	50	0.152
	51	0.180
	52	0.161
	53	0.155
	54	0.137
	55	0.126
	56	0.117
	57	0.118
	58	0.127
	59	0.137
	60	0.177
	61	0.188
	62	0.167

Table 3
Thickness Measurements From the Field Cut End of T3
From Locations Indicated in Figure 4

Sample Region	Location Number	Wall Thickness (inch)
T3 Cut End	63	0.295
	64	0.302
	65	0.333
	66	0.299

Table 4
Thickness Measurement Results from the T4 Side of the T1 to T4 Rupture and the Cut End of T4
From Locations Indicated in Figure 5b and Figure 5c

Sample Region	Location Number	Wall Thickness (inch)
T4 Side of T1-T4 Fracture	136	0.287
	137	0.287
	138	0.294
	139	0.301
	140	0.302
	141	0.300
	142	0.285
	143	0.281
	144	0.278
	145	0.275
	146	0.278
	147	0.277

Sample Region	Location Number	Wall Thickness (inch)
T4 Cut End	148	0.328
	149	0.296
	150	0.302
	151	0.303
	152	0.292
	153	0.314
	154	0.293
	155	0.294
	156	0.289
	157	0.300
	158	0.300
	159	0.314

Table 5
Thickness Measurement Results for the Longitudinal Section Through T1
From the Locations Indicated in Figure 7

Sample Region	Location Number	Wall Thickness (inch)
T2 Inside Bend	68	0.337
	69	0.339
	70	0.304
T1 Inside Bend	71	0.171
	72	0.174
	73	0.213
	74	0.218
	75	0.223
	76	0.231
	77	0.222
	78	0.201
	79	0.192
	80	0.178
	81	0.149
T2 Outside Bend	82	0.347
	83	0.346
	84	0.344
	85	0.198
T1 Outside Bend	86	0.170
	87	0.150
	88	0.128
	89	0.110
	90	0.100
	91	0.091
	92	0.085
	93	0.066
	94	0.053
	95	0.044
	96	0.055
	97	0.090
	98	0.114
	99	0.134
	100	0.154
	101	0.158
	102	0.161
	103	0.162

Table 6
Thickness Measurement Results for the Longitudinal Section Through T2
From the Locations Indicated in Figure 8

Sample Region	Location Number	Wall Thickness (inch)
T3	104	0.290
Weld	105	0.307
T2 Inside Bend	106	0.313
	107	0.344
	108	0.360
	109	0.377
	110	0.379
	111	0.385
	112	0.381
	113	0.375
	114	0.370
T3	115	0.287
Weld	116	0.479
T2 Outside Bend	117	0.362
	118	0.355
	119	0.349
	120	0.332
	121	0.323
	122	0.304
	123	0.311
	124	0.305
	125	0.302
	126	0.293
	127	0.288
	128	0.295
	129	0.288
	130	0.282
	131	0.275
	132	0.283
	133	0.285
	134	0.283
	135	0.293

Table 7
Quantitative Chemical Analysis Results for
Elbow T1 and Elbow T2, Compared to the Chemical Composition Requirements of
ASTM A 106-68, Grade B Carbon Steel and Yoloy Steel[15]

Element		T1 (wt%)	T2 (wt%)	Requirements for ASTM A 106-68 Grade B (wt%)		Requirements for Yoloy Steel (wt%)	
				min	min	max	max
Carbon[A]	(C)	0.14	0.24	-.-	0.30		0.25
Manganese	(Mn)	0.80	0.90	0.29	1.06	Infomation	
Phosphorus	(P)	≤0.005	0.012	-.-	0.048	Information	
Sulfur[A]	(S)	0.010	0.016	-.-	0.058	Information	
Silicon	(Si)	0.10	0.24	0.10	-.-	Information	
Iron	(Fe)	Primary Constituent					
Chromium	(Cr)	0.18	0.02	Information		Information	
Molybdenum	(Mo)	0.06	<0.005	Information		Information	
Nickel	(Ni)	1.74	≤0.01	Information		-.-	2.0
Copper	(Cu)	0.84	0.02	Information		-.-	1.0
Vanadium	(V)	<0.005	<0.005	Information		Information	
Niobium	(Nb)	<0.005	<0.005	Information		Information	
Titanium	(Ti)	<0.005	<0.005	Information		Information	
Aluminum	(Al)	0.08	0.04	Information		Information	
Cu +Ni		2.58	0.03	Information		Information	
Carbon Equivalent		<0.49	≤0.40	Information		Information	

[A] Concentration determined by LECO combustion
Concentration of all other elements determined by spark optical emission spectroscopy
Carbon Equivalent (CE) = C + Mn/6 + (Cr+Mo+V)/5 + (Ni+Cu)/15

[15] SYMPOSIUM ON HIGH-STRENGTH CONSTRUCTIONAL METALS, AMERICAN SOCIETY FOR TESTING MATERIALS, March 4, 1936, P. 13.

Table 8
Quantitative Chemical Analysis Results for
Pipe T3 and Pipe T4 Compared to the Chemical Composition Requirements of
ASTM A 106-68, Grade B Carbon Steel

Element	Pipe T3 (wt%)	Pipe T4 (wt%)	Requirements for ASTM A 106-68 Grade B (wt%)	
			min	max
Carbon[A] (C)	0.25	0.25	-.-	0.30
Manganese (Mn)	0.58	0.57	0.29	1.06
Phosphorus (P)	0.007	0.007	-.-	0.048
Sulfur[A] (S)	0.018	0.015	-.-	0.058
Silicon (Si)	0.18	0.17	0.10	-.-
Iron (Fe)	Primary Constituent			
Chromium (Cr)	<0.01	0.01	Information	
Molybdenum (Mo)	≤0.005	≤0.005	Information	
Nickel (Ni)	<0.01	≤0.01	Information	
Copper (Cu)	<0.01	<0.01	Information	
Vanadium (V)	<0.005	<0.005	Information	
Niobium (Nb)	<0.01	<0.005	Information	
Titanium (Ti)	<0.005	<0.005	Information	
Aluminum (Al)	0.01	0.01	Information	
Cu +Ni	0.02	0.02	Information	
Carbon Equivalent	≤0.35	≤0.35	Information	

[A] Concentration determined by LECO combustion
Concentration of all other elements determined by spark optical emission spectroscopy
Carbon Equivalent (CE) = C + Mn/6 + (Cr+Mo+V)/5 + (Ni+Cu)/15

Table 9
Quantitative Chemical Analysis Results for
Weld Metal Compared to the Chemical Composition Requirements
of ASTM 106-68, Grade B Carbon Steel

Element		T1-T2 Weld (wt%)	T1-T4 Weld (wt%)	T2-T3 Weld (wt%)	Requirements for ASTM A 106-68 Grade B (wt%)	
					min	max
Carbon[A]	(C)	0.13	0.062	0.11	-.-	0.30
Manganese	(Mn)	1.02	1.20	0.99	0.29	1.06
Phosphorus	(P)	0.011	0.024	0.008	-.-	0.048
Sulfur[A]	(S)	0.020	0.024	0.020	-.-	0.058
Silicon	(Si)	0.52	0.45	0.56	0.10	-.-
Iron	(Fe)	Primary Constituent				
Chromium	(Cr)	0.06	0.04	0.02	Information	
Copper	(Cu)	0.25	0.19	0.05	Information	
Molybdenum	(Mo)	0.01	0.01	≤0.005	Information	
Nickel	(Ni)	0.21	0.19	0.02	Information	
Vanadium	(V)	<0.005	≤0.005	0.02	Information	
Niobium	(Nb)	<0.01	≤0.01	≤0.01	Information	
Titanium	(Ti)	<0.005	<0.005	≤0.01	Information	
Aluminum	(Al)	0.01	0.01	<0.01	Information	
Cu + Ni + Cr		0.52	0.42	0.09	Information	
Carbon Equivalent		0.35	0.30	0.29	Information	

[A] Concentration of C and S determined by LECO combustion
Concentration of all other elements determined by spark optical emission spectroscopy
Carbon Equivalent (CE) = C + Mn/6 + (Cr+Mo+V)/5 + (Ni+Cu)/15

Table 10
Chemical Composition Requirements from Year 2015 Versions of
ASTM A234 and ASTM A106

Element		Requirements for ASTM A234-15 Grade WPB (wt%)		Requirements for ASTM 106-15 Grade WPB (wt%)	
		min	max	min	max
Carbon	(C)	0.18	0.30	0.18	0.30
Manganese	(Mn)	0.29	1.06	0.29	1.06
Phosphorus	(P)	-.-	0.035	-.-	0.035
Sulfur	(S)	-.-	0.035	-.-	0.035
Silicon	(Si)	0.10	-.-	0.10	-.-
Chromium	(Cr)	-.-	0.40	-.-	0.40
Copper	(Cu)	-.-	0.40	-.-	0.40
Molybdenum	(Mo)	-.-	0.15	-.-	0.15
Nickel	(Ni)	-.-	0.40	-.-	0.40
Vanadium[A]	(V)	-.-	0.03	-.-	0.02
Niobium[A]	(Nb)	-.-	0.02	-.-	0.02
Cu+Ni+Cr+Mo		-.-	1.00	-.-	-.-
Cr+Cu+Mo+Ni+V		-.-	-.-	-.-	1.00
V+Nb[A]		-.-	-.-	-.-	0.03
Ni+Cu[A]		-.-	-.-	-.-	0.15
Titanium	(Ti)	Information			
Aluminum	(Al)	Information			
Carbon Equivalent		-.-	0.50	-.-	0.43

[A] Supplementary requirements
Carbon Equivalent (CE) = C + Mn/6 + (Cr+Mo+V)/5 + (Ni+Cu)/15

Table 11
Chemical Analysis Results for Internal Scale Scraped from T1, T3 and T4

Specimen Location	Fluorine Detected By EDS	Chemical Composition By XRD	Abundance By XRD (wt%)
T1 extrados friable scale	X		
T1 extrados scrapings tenacious scale	X	Fe_2O_3 $Cu_{0.86}Fe_{2.14}O_4$ SiO_2 FeO(OH) CaF_2	62.9 15.3 10.7 6.7 4.5
T1 at thickness location 51 to 52	X	Fe_2O_3 FeO(OH) $CuFeS_2$ $Cu_{0.86}Fe_{2.14}O_4$	74.2 10.4 8.8 6.5
T4 1-inch inside fractured end	X		
T4 8-inches inside fractured end	X	$Fe_{2.67}O_4$ FeO(OH) $Fe_4O_4(OH)_{0.8}F_{3.2}•0.8H_2O$ Si	46.7 36.8 10.0 6.5
T3 cut end thickness location 63	X	$Fe_2F_5•7H_2O$ $FeF_2(H_2O)_4$ FeO(OH)	80.2 10.8 9.0
T3 cut end thickness location 65	X		
T4 cut end	X	$Fe_2F_5•7H_2O$ $Fe_4O_4(OH)_{0.8}F_{3.2}•0.8H_2O$ $FeF_3•3H_2O$ $FeF_3•0.33H_2O$ Unidentified phases	86.6 9.2 4.0 0.1 0.1

Table 12
Knoop 0.500-kg Hardness Test Results from Section of Weld T1-T2 Prepared for Metallography

Indent	Region	Result (HK)	Converted[A] Brinell Hardness (HBS)
1	Weld	196.3	213
2	T1 FZ	216.2	235
3	T1 HAZ	215.5	234
4		232.0	252
5		240.5	261
6		229.2	249
7		238.5	258
8	Weld	178.2	194
9	T2 HAZ	194.8	212
10		173.3	189
11		183.1	199
12		142.3	156
13		189.2	206
14		199.4	217

[A] Knoop hardness converted to Brinell hardness according to E140-12, Table 2
Fusion zone (FZ)
Heat affected zone (HAZ)

Table 13
Knoop 500-g Hardness Test Results from Section of Weld T2-T3 Prepared for Metallography

Indent	Region	Result (HK500)	Converted[A] Brinell Hardness (HBS)
1	Weld	183.7	200
2	T2 FZ	200.9	218
3	T2 HAZ	200.9	218
4		193.2	210
5		195.6	213
6		202.6	220
7		204.1	222
8	Weld	199.6	217
9		203.9	222
10	T3 HAZ	199.4	217
11		189.0	206
12		163.8	179
13		166.8	182
14		155.4	170

[A] Knoop hardness converted to Brinell hardness according to E140-12, Table 2
Fusion zone (FZ)
Heat affected zone (HAZ)

Table 14
Knoop 500-g Hardness Test Results from Section of Weld T1-T4 Prepared for Metallography

Indent	Region	Result (HK500)	Converted[A] Brinell Hardness (HBS)
1	Weld	153.9	168
2		157.4	172
3		153.2	168
4	T1 FZ	207.2	225
5	T1 HAZ	255.1	276
6		272.8	295
7		257.6	279
8		310.4	335
9		206.5	224
10		203.9	222
11		200.0	217
12		201.1	219
13	Weld	150.3	164
14		153.2	168
15		158.9	174
16	T4 FZ	153.5	168
17	T4 HAZ	164.6	180
18		164.1	179
19		157.7	172
20		168.0	183
21		156.7	171
22		142.9	157
23		157.3	172

[A] Knoop hardness converted to Brinell hardness according to E140-12, Table 2
Fusion zone (FZ)
Heat affected zone (HAZ)

Table 15
Tensile Test Results for Specimens Machined from T3 Pipe

		Specimen 1	Specimen 2	Specimen 3	A 106-68 Grade B
Tensile strength	(psi)	69600	69400	68600	60000
Yield point	(psi)	43300	45900	43000	36000
Elongation in 2-inch gage	(%)	28	31	31	30

Table 16
Charpy V-Notch Impact Toughness Results for Specimens 6-mm x 10-mm x 55-mm
Machined from T3 Pipe

Specimen	Energy Absorbed (ft•lbs)	Lateral Expansion (mils)	Fracture Apperance Shea (%)r
1	19.2	43	55
2	19.5	40	57
3	20.6	42	60
Average	19.8	41.7	57.3

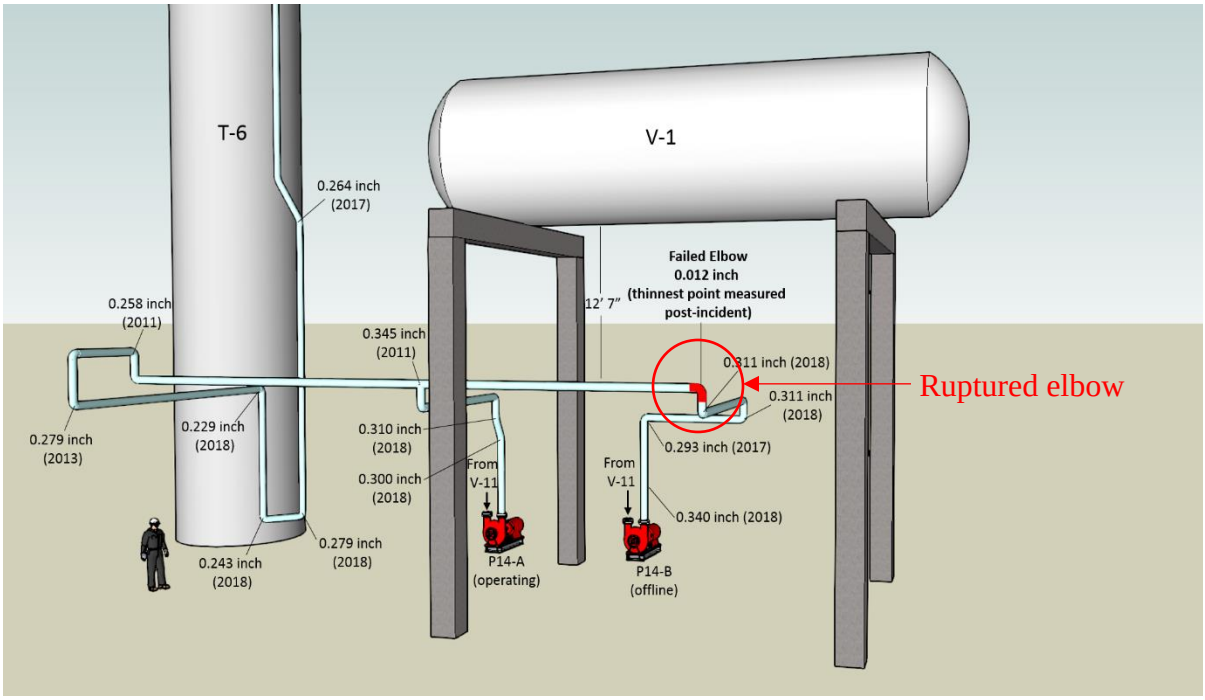

(a) Credit: CSB

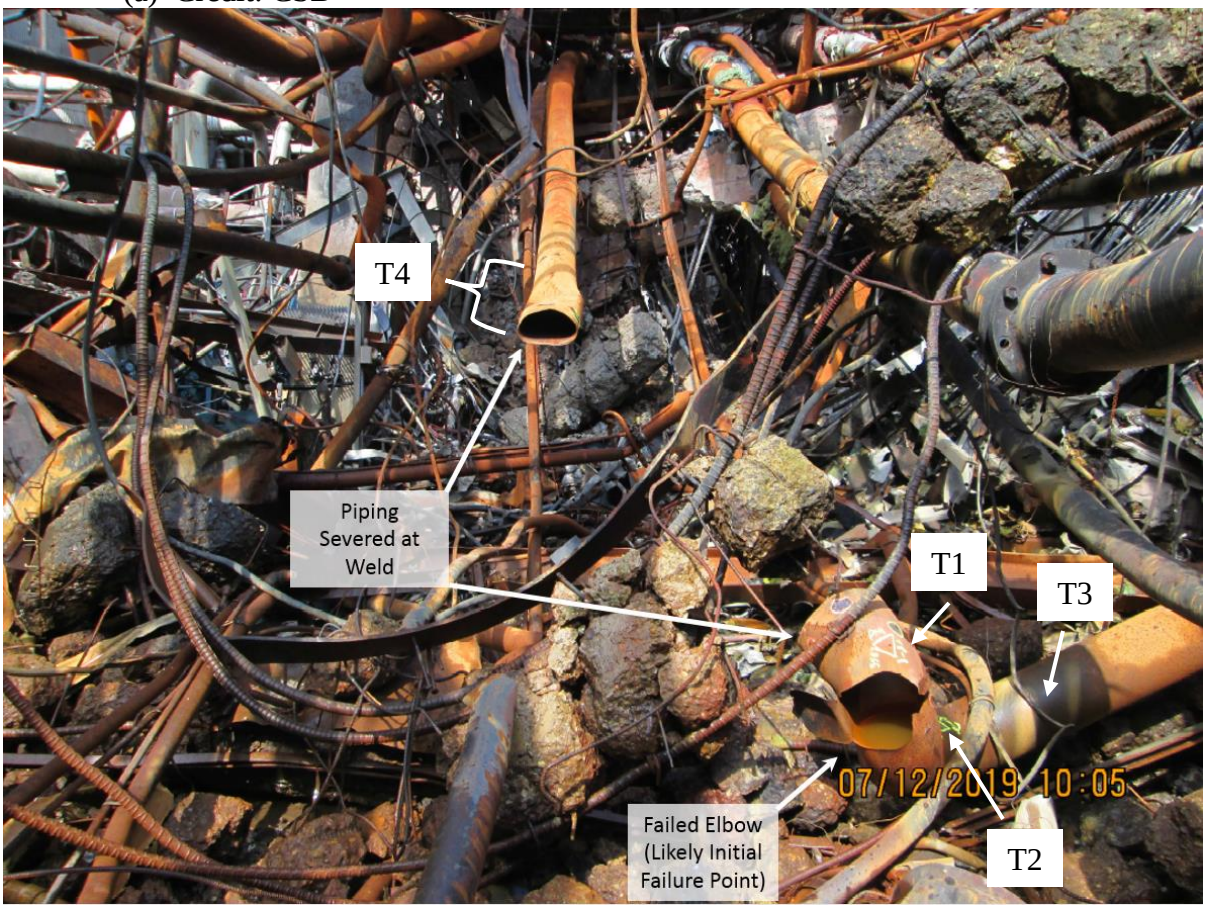

(b) Credit: CSB and PES

Figure 1 Model of the subject ruptured line in relationship to T-6 and V-1, and a post incident photograph of the ruptured elbow and fractured girth weld.

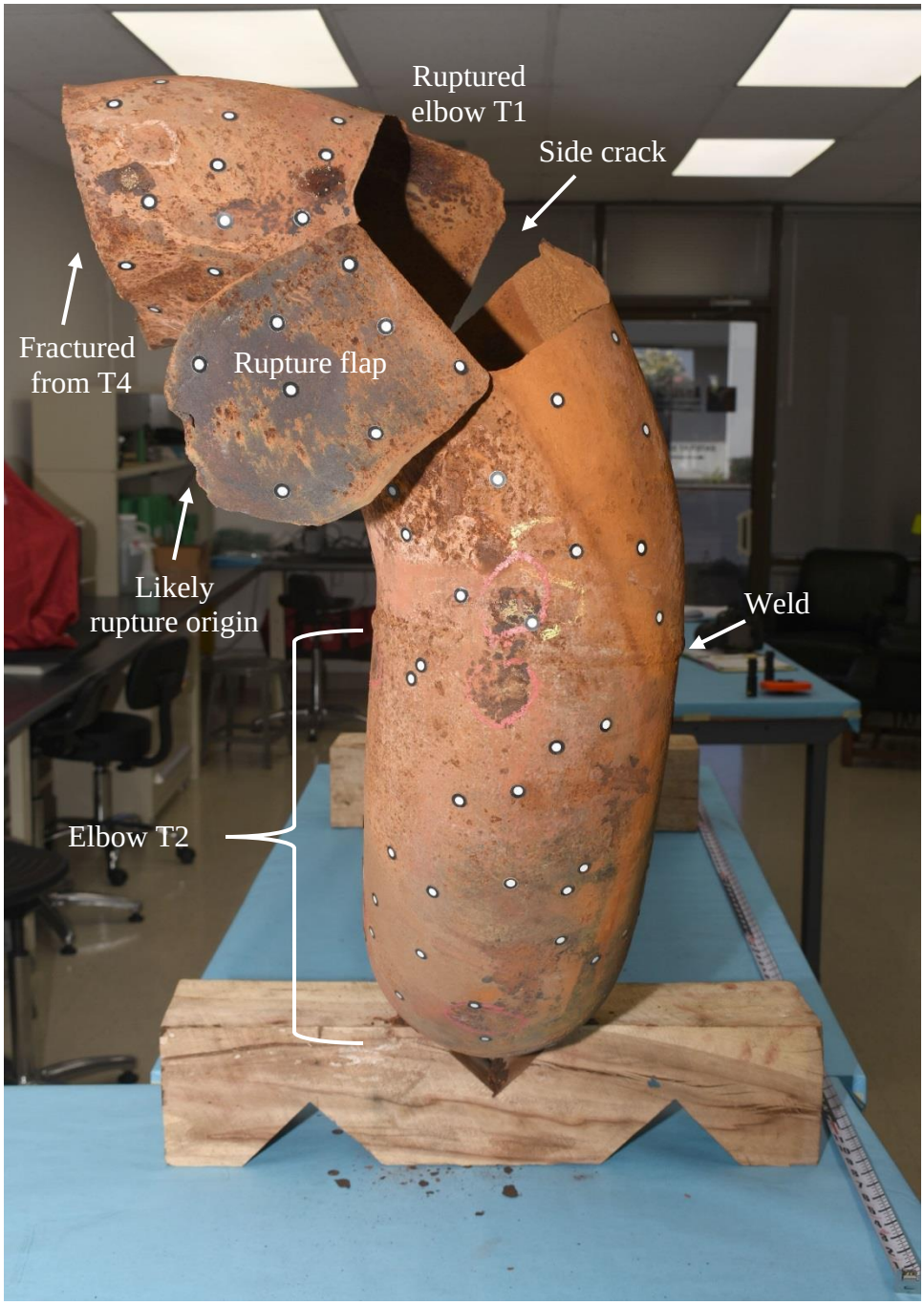

Figure 2 Photograph of E004, viewed from the ruptured end. Spots are reflectors that were applied to facilitate laser scanning.

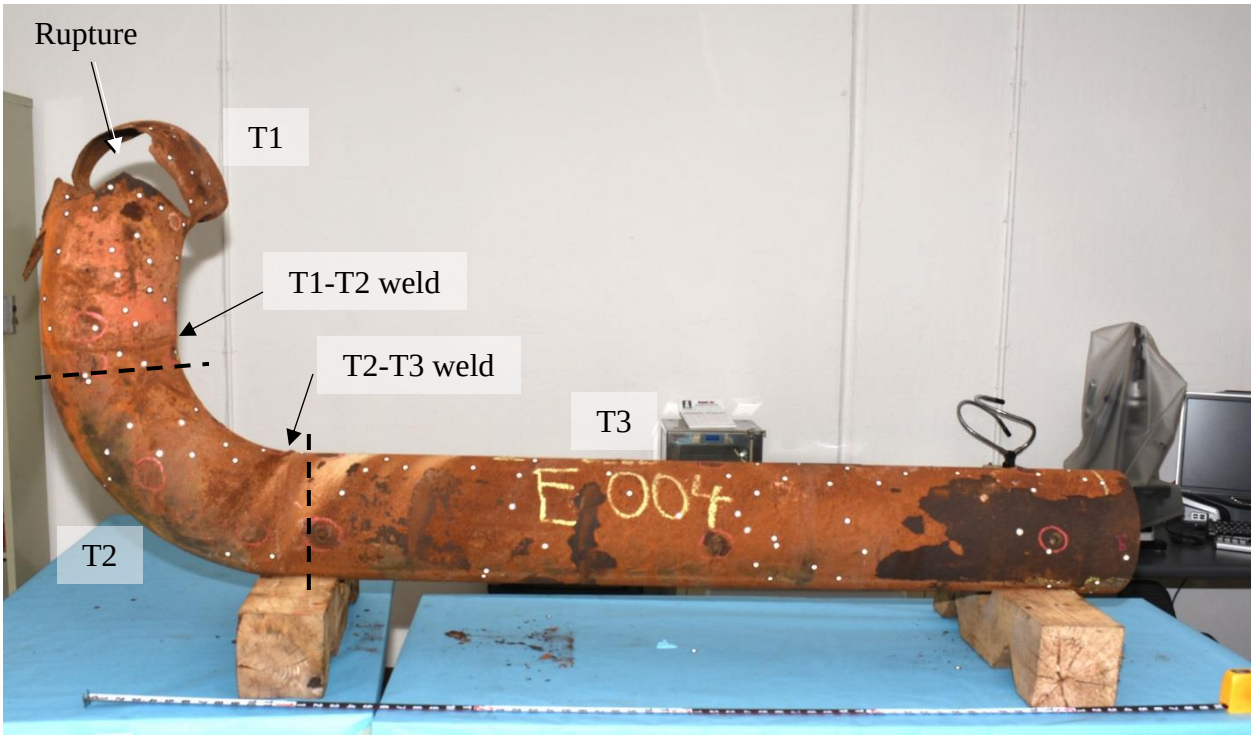

(a)

(b)

Figure 3 Photographs of E004. Spots are reflectors that were applied prior to laser scanning. Dashed lines in (a) indicate transverse cut locations.

Figure 4 Photograph of E004, viewed from the cut end of T3. Spots are reflectors that were applied prior to laser scanning. Numbers at the cut end indicate locations of wall thickness measurements listed in Table 3.

(a)

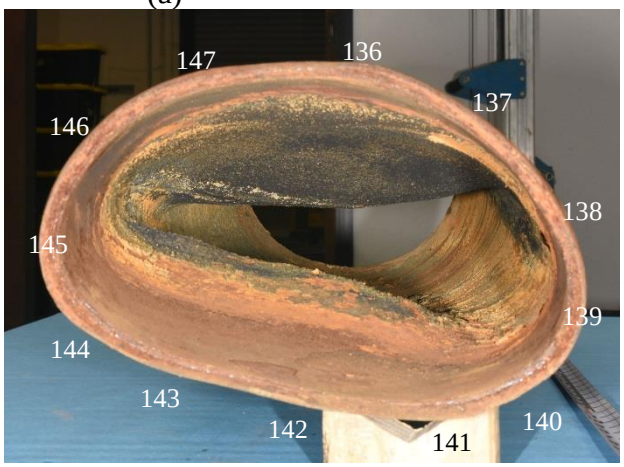

(b) Fractured end

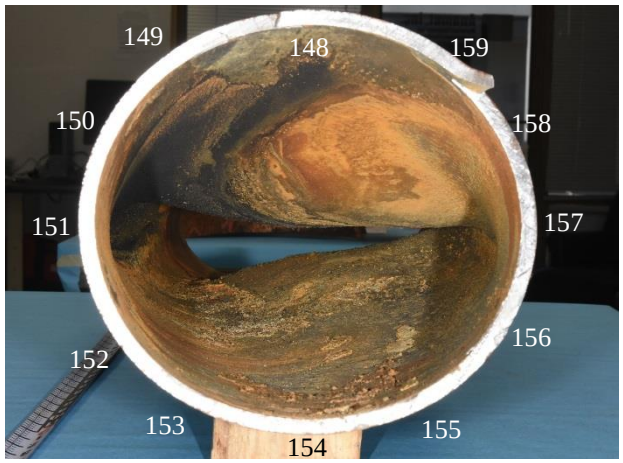

(c) Cut end

Figure 5 Photographs of E012, referred to as T4. Numbers in (b) and (c) indicate locations of wall thickness measurements listed in Table 4.

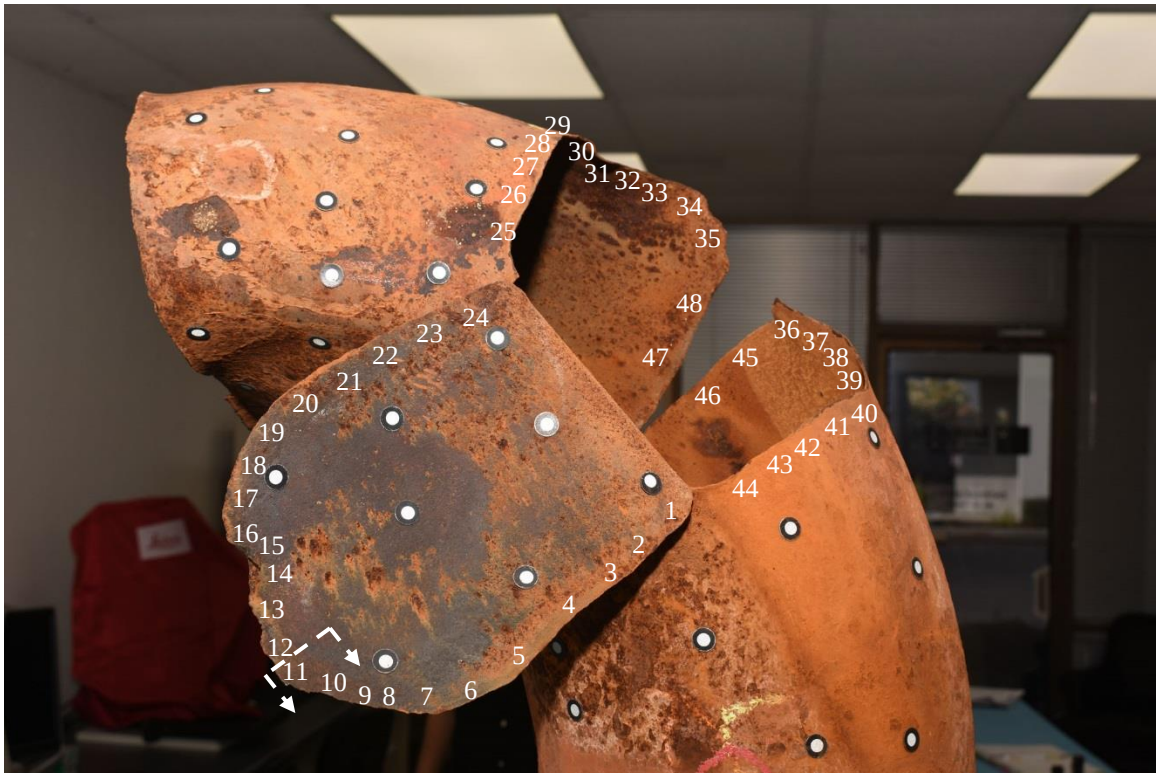

(a)

(b)

Figure 6 Photographs of ruptured elbow T1. Numbers indicate thickness measurement locations indicated in Table 1 and Table 2. Dashed lines in (a) between location 11 and 12 indicate a section prepared for metallography.

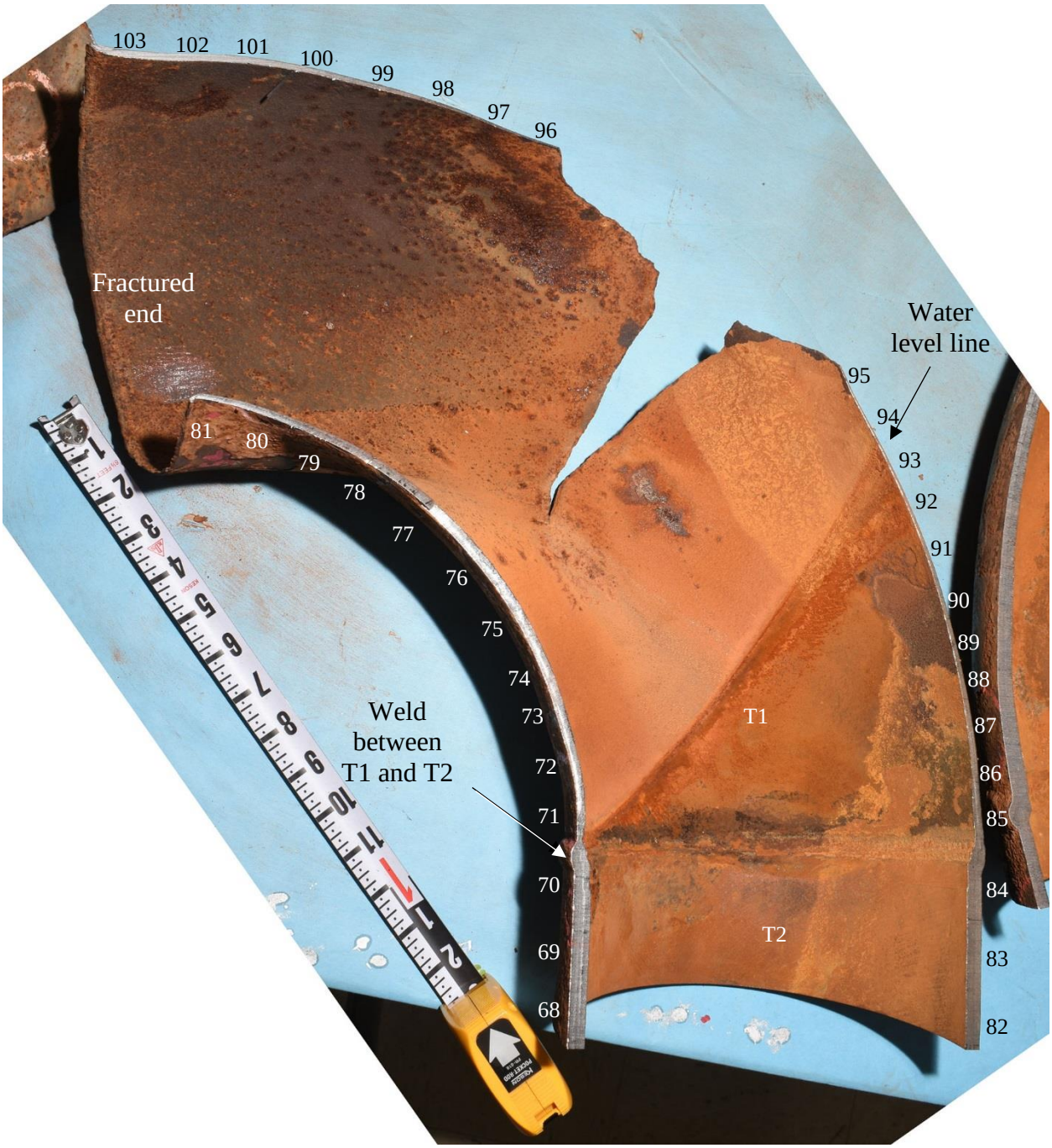

Figure 7 Longitudinal section of ruptured elbow T1. Numbers indicate thickness measurement locations listed in Table 5.

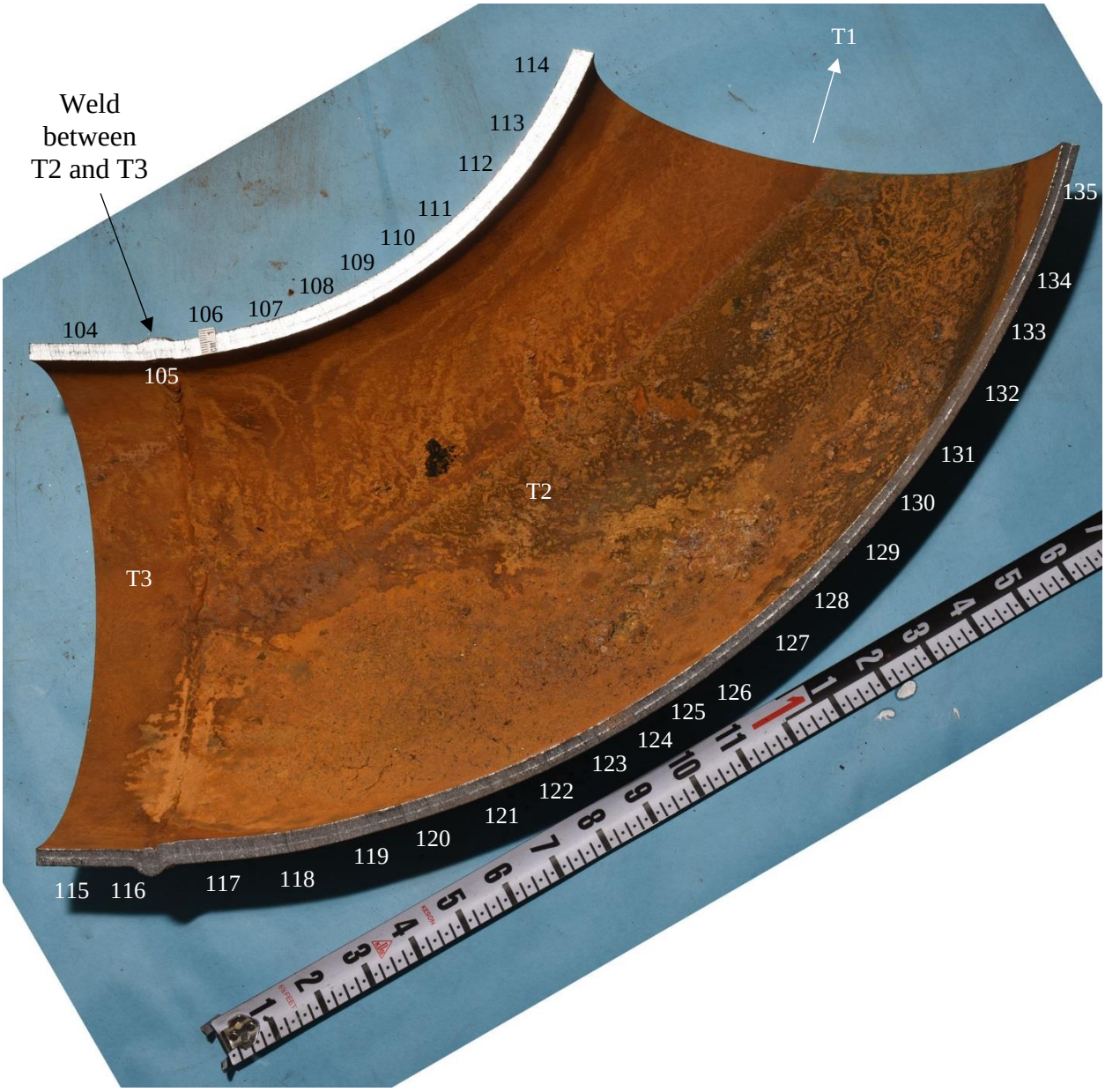

Figure 8 Longitudinal section through elbow T2.. Numbers indicate thickness measurement locations listed in Table 6.

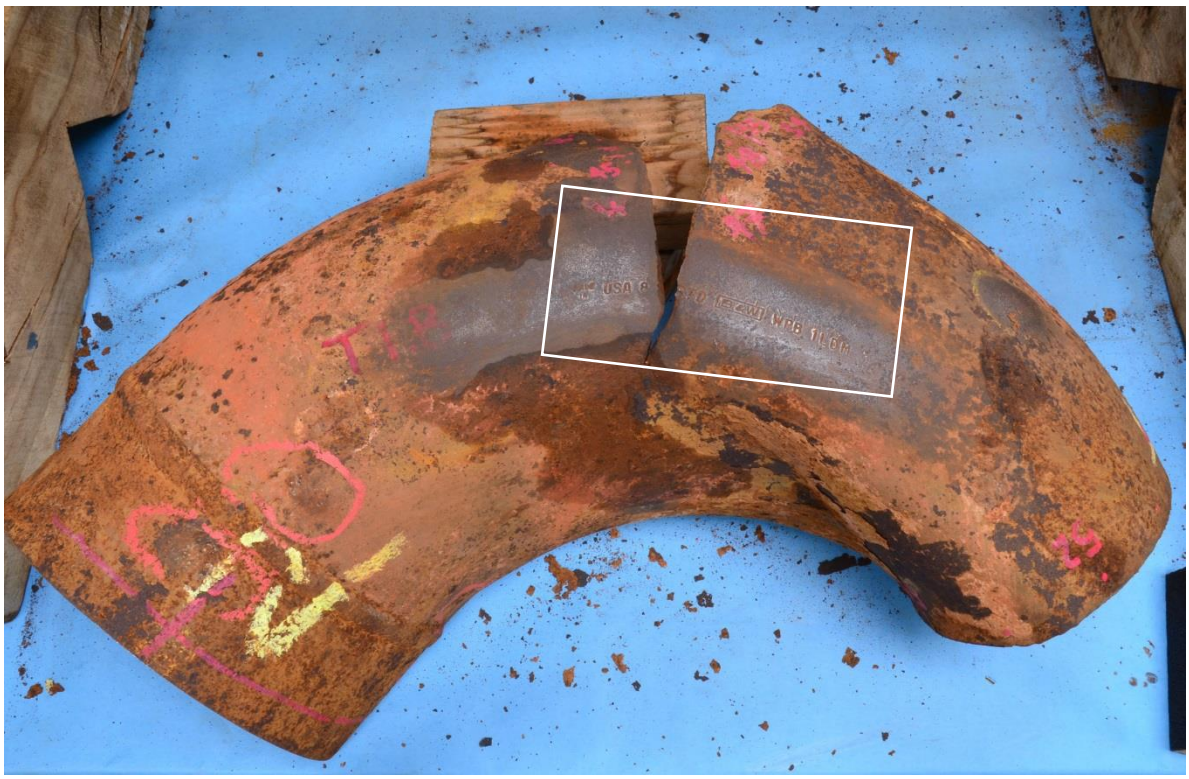

(a)

(b) Boxed region in (a)

Figure 9 Photographs of the stamped surface of the ruptured elbow T1 after removing corrosion scale with a grinding pad.

(a) Prior to cleaning

(b) After cleaning, boxed region in (a)

Figure 10 Photographs of elbow T2. In (a), stamps are shown after removing corrosion scale with a grinding pad.

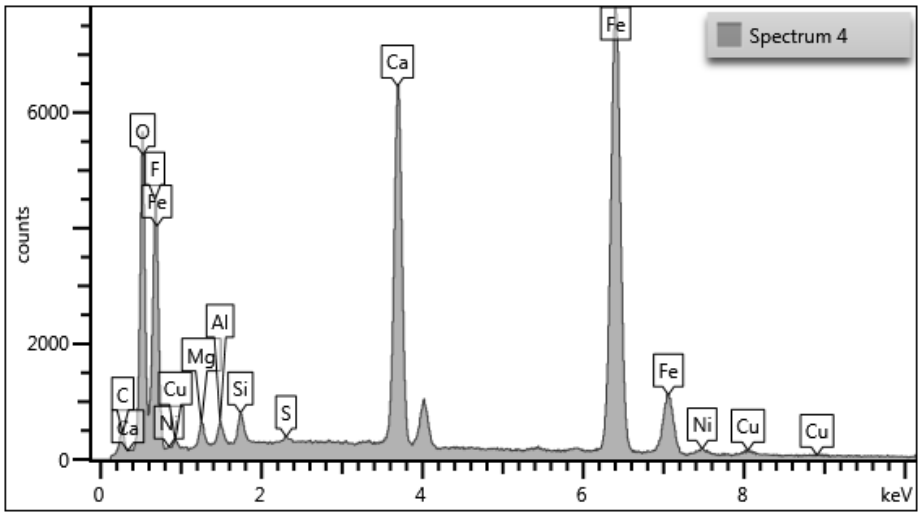

(a) Tenacious scale from inside T1 extrados

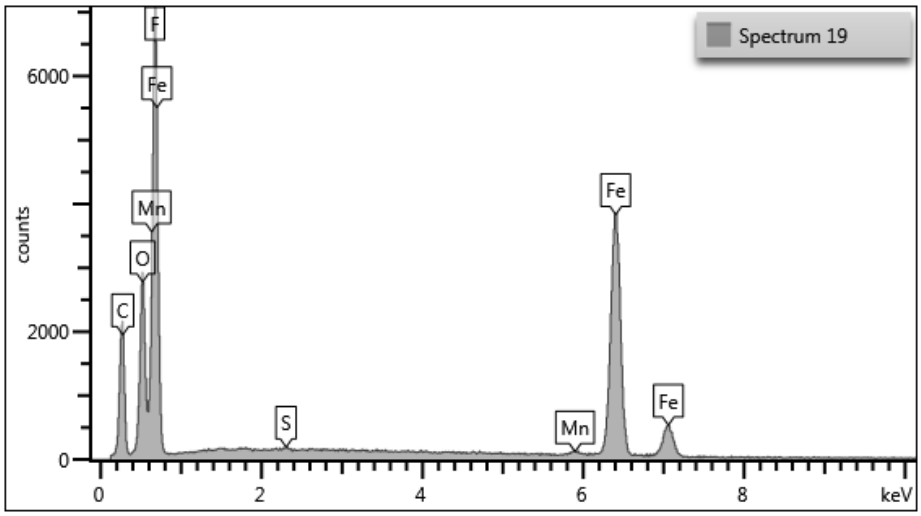

(b) Tenacious scale from inside T3 cut end, thickness location 63

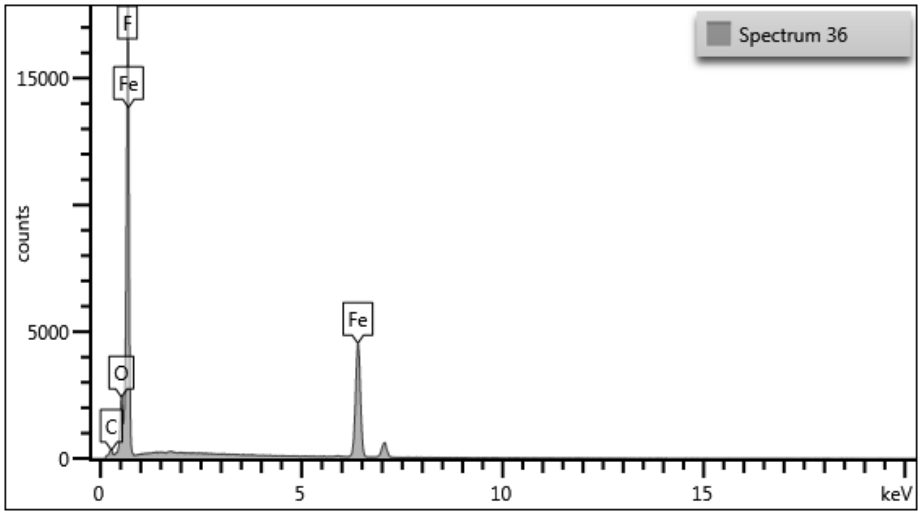

(c) Tenacious scale from inside T1 extrados

Figure 11 Representative EDS spectra.

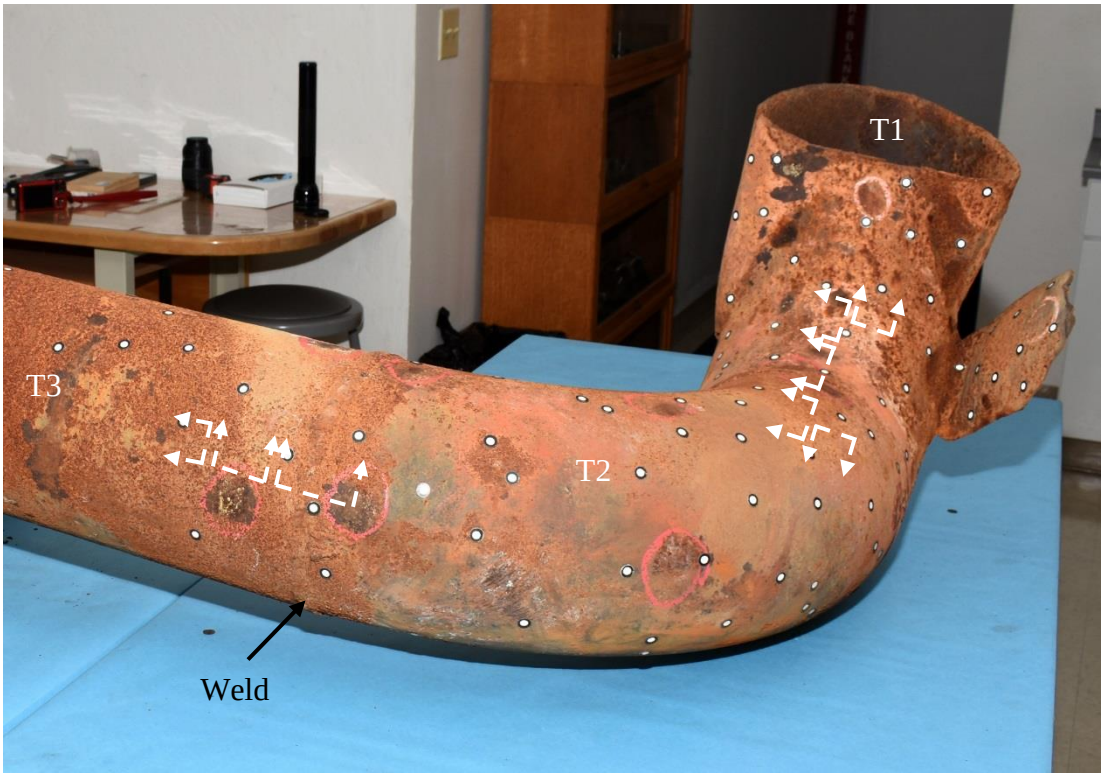

(a)

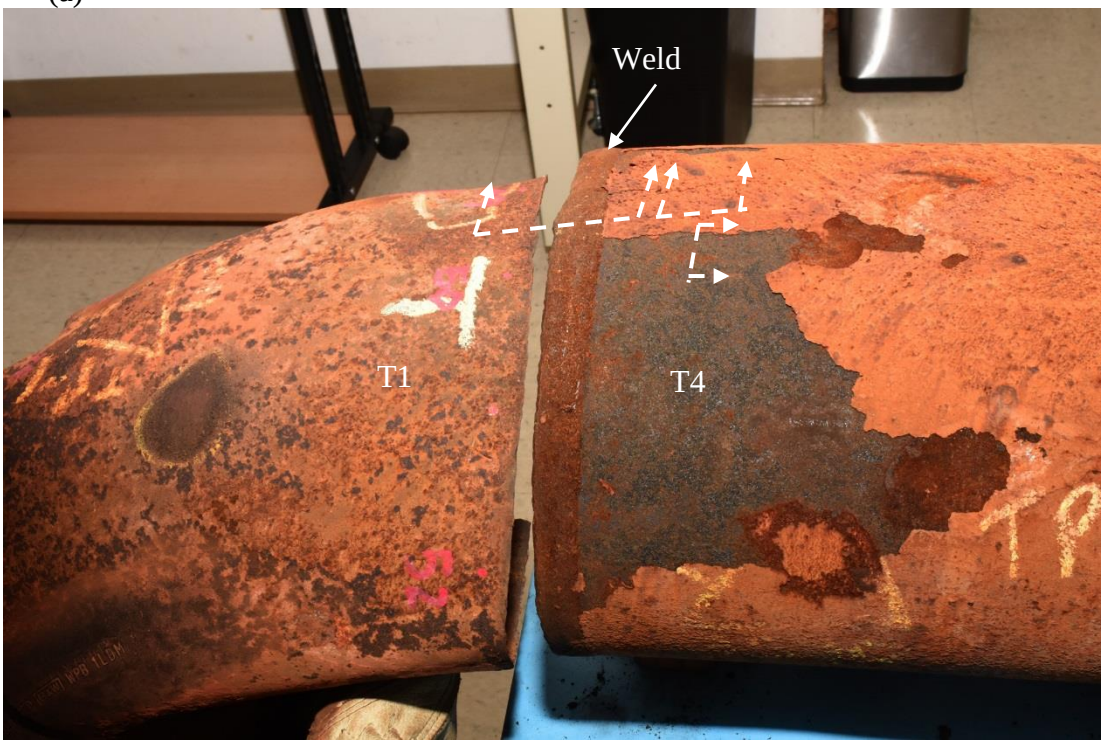

(b)

Figure 12 Photographs of the locations from which sections were cut for metallography.

Figure 13 Photograph of the longitudinal section through the T1 to T2 weld prepared for metallography.

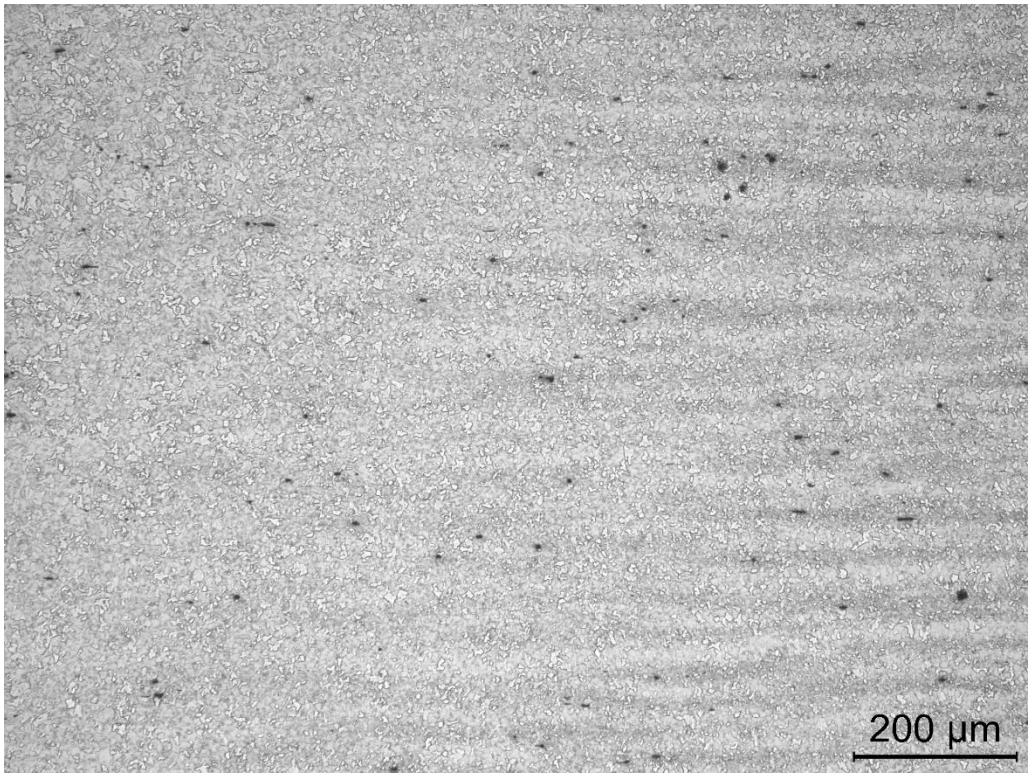

(a) 100X

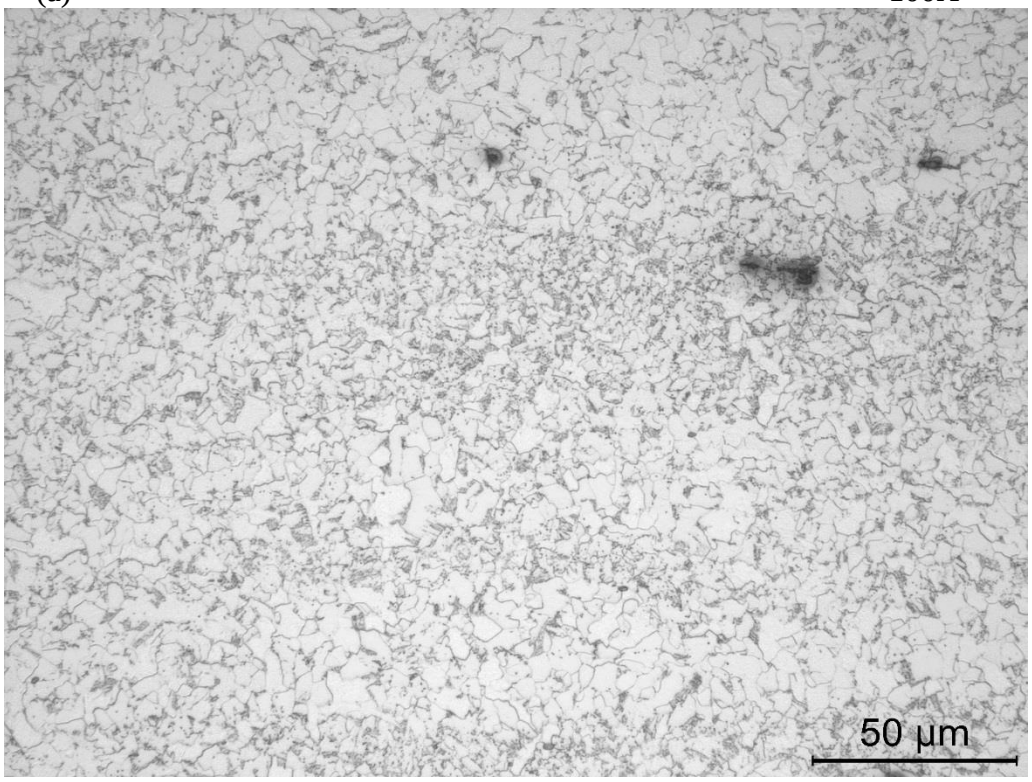

(b) 500X

Figure 14 Micrographs of the T1 weld heat affected zone, from the boxed region α in Figure 13.

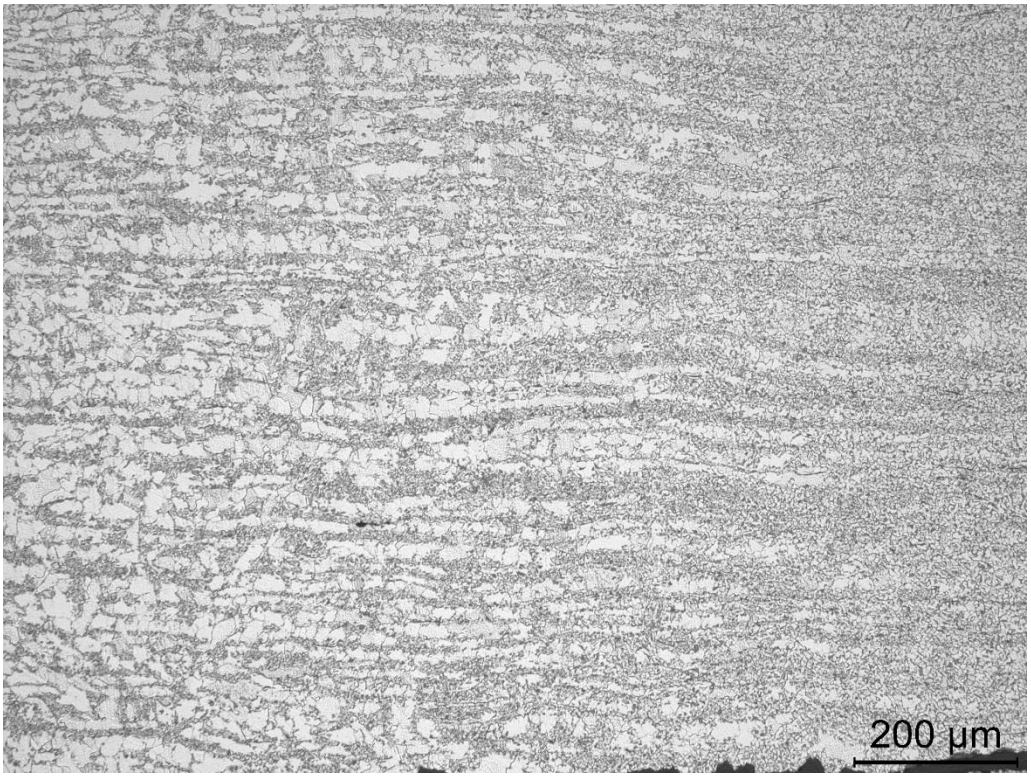

(a) 100X

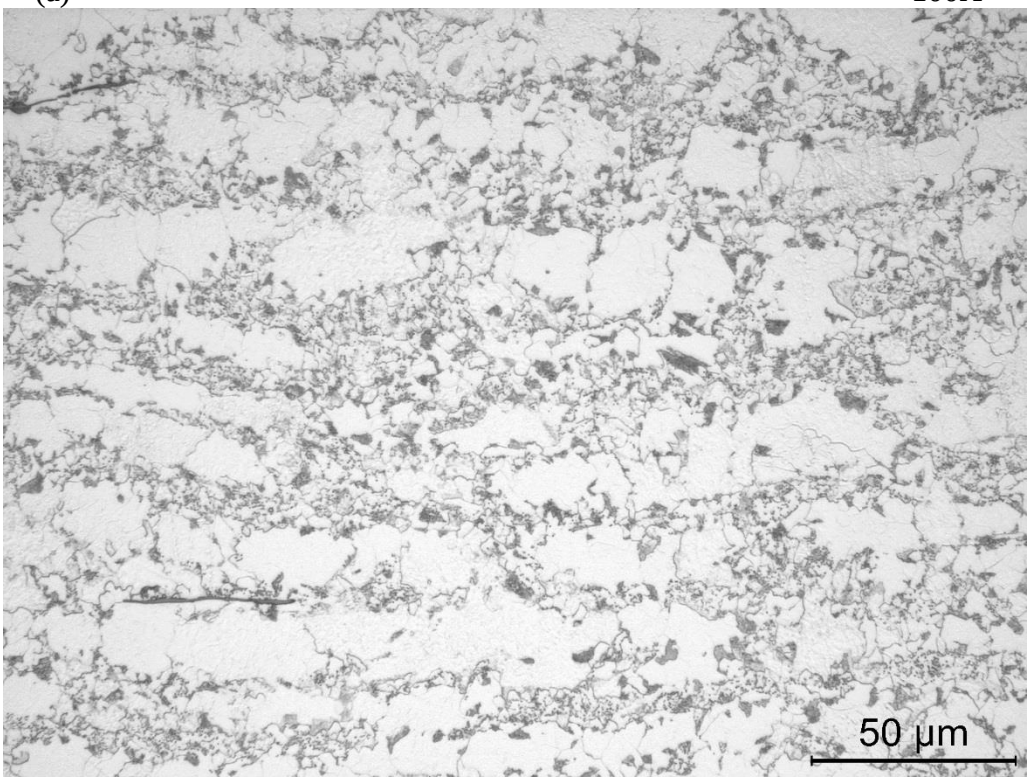

(b) 500X

Figure 15 Micrographs of the T2 weld heat affected zone. from the boxed region β in Figure 13.

Figure 16 Photograph of the longitudinal section through the T1 to T4 weld prepared for metallography.

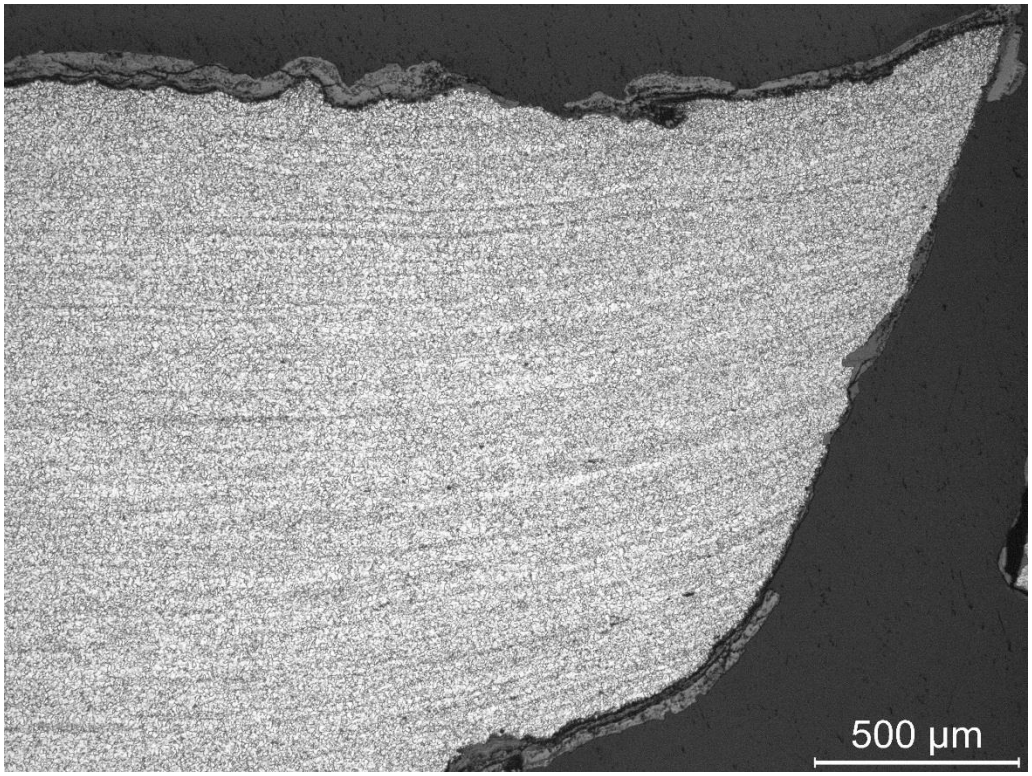

(a) 13X

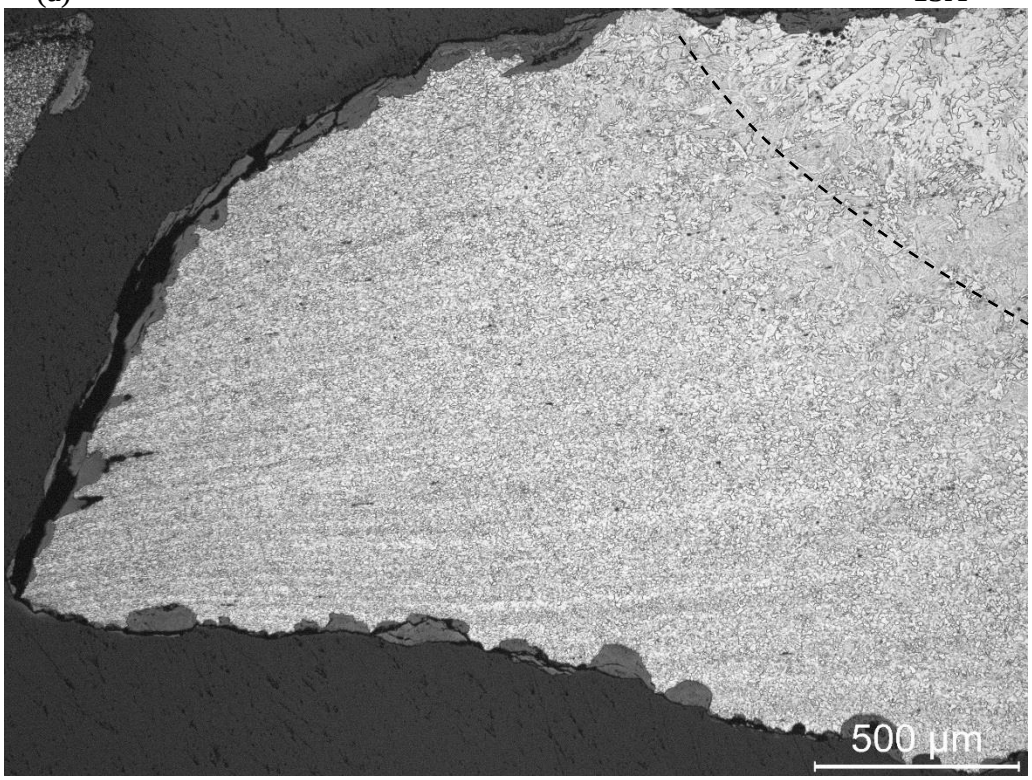

(b) 13X

Figure 17 Micrographs of the section through T1 to T4 weld. The dashed line in (b) indicates the weld fusion zone on the T1 side of the joint.

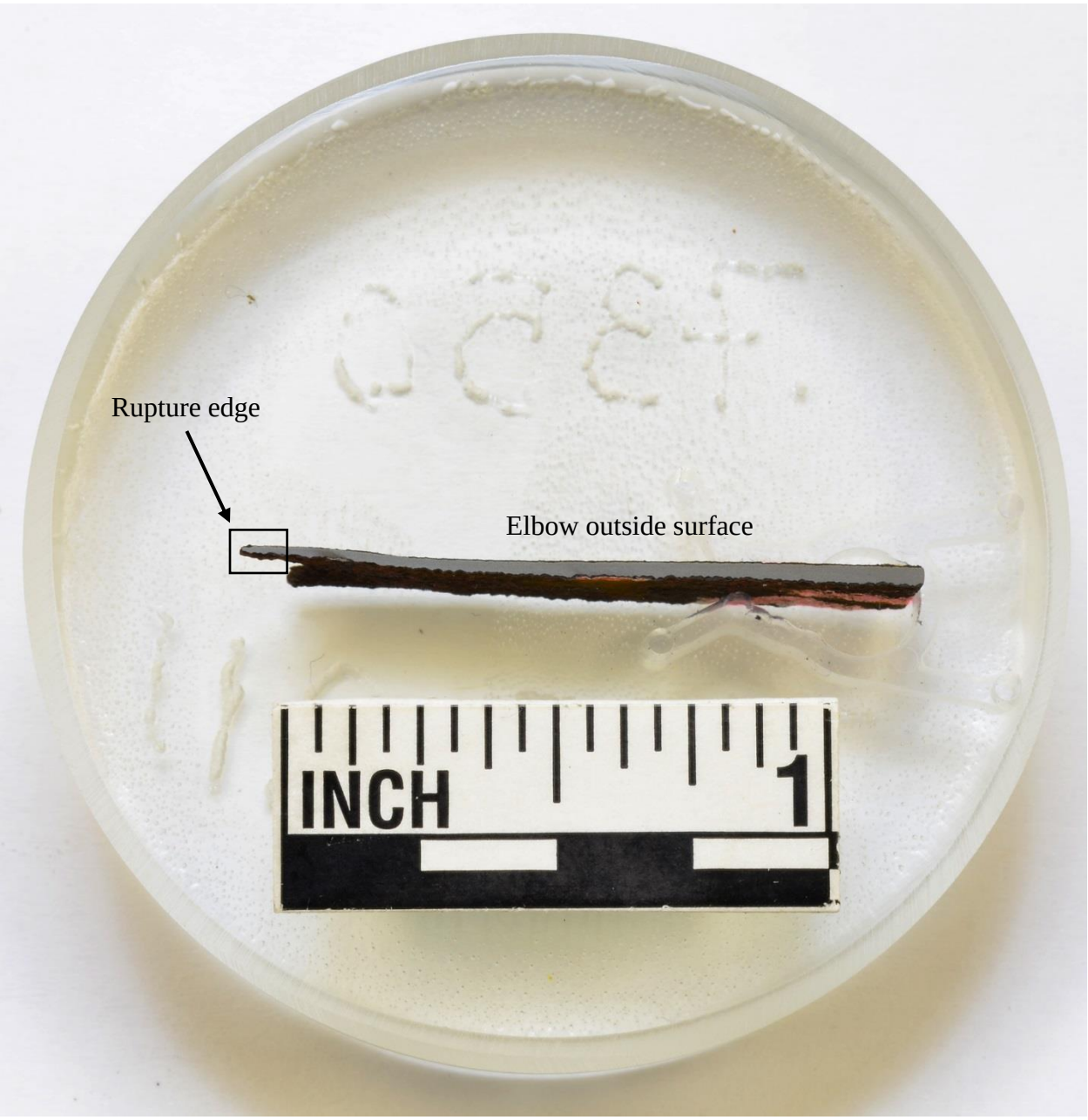

Figure 18 Photograph of the rupture flap section prepared for metallography.

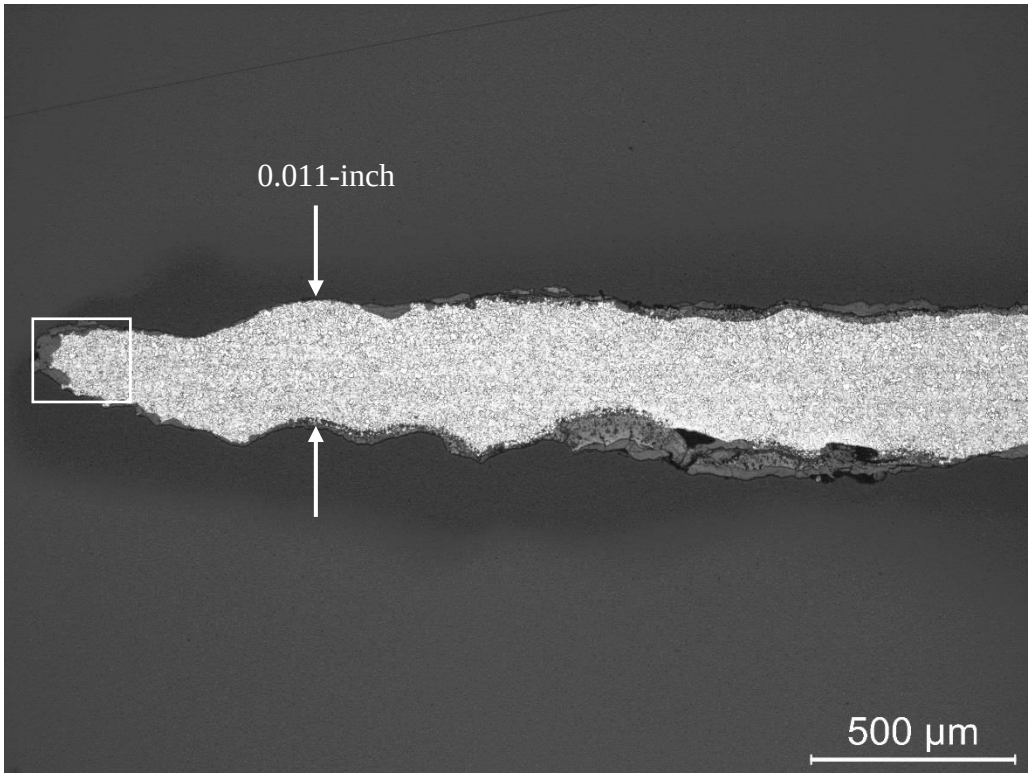

(a) 50X

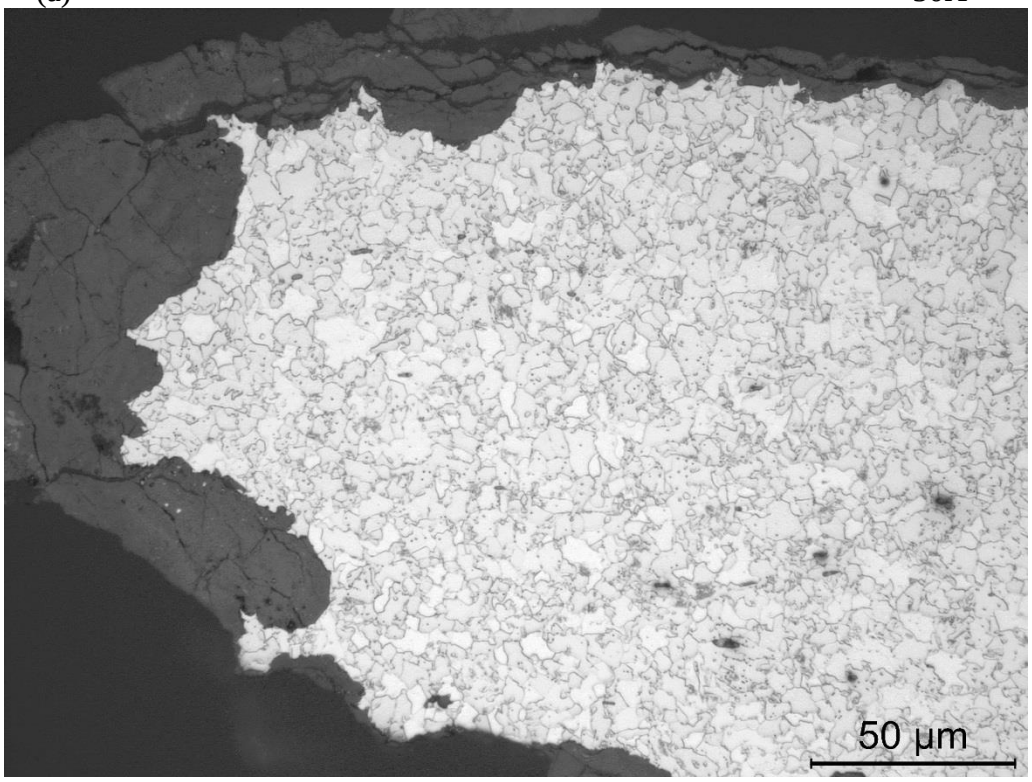

(b) Boxed region in (a) 500X

Figure 19 Micrographs of the rupture flap section prepared for metallography, from the boxed region in Figure 18.

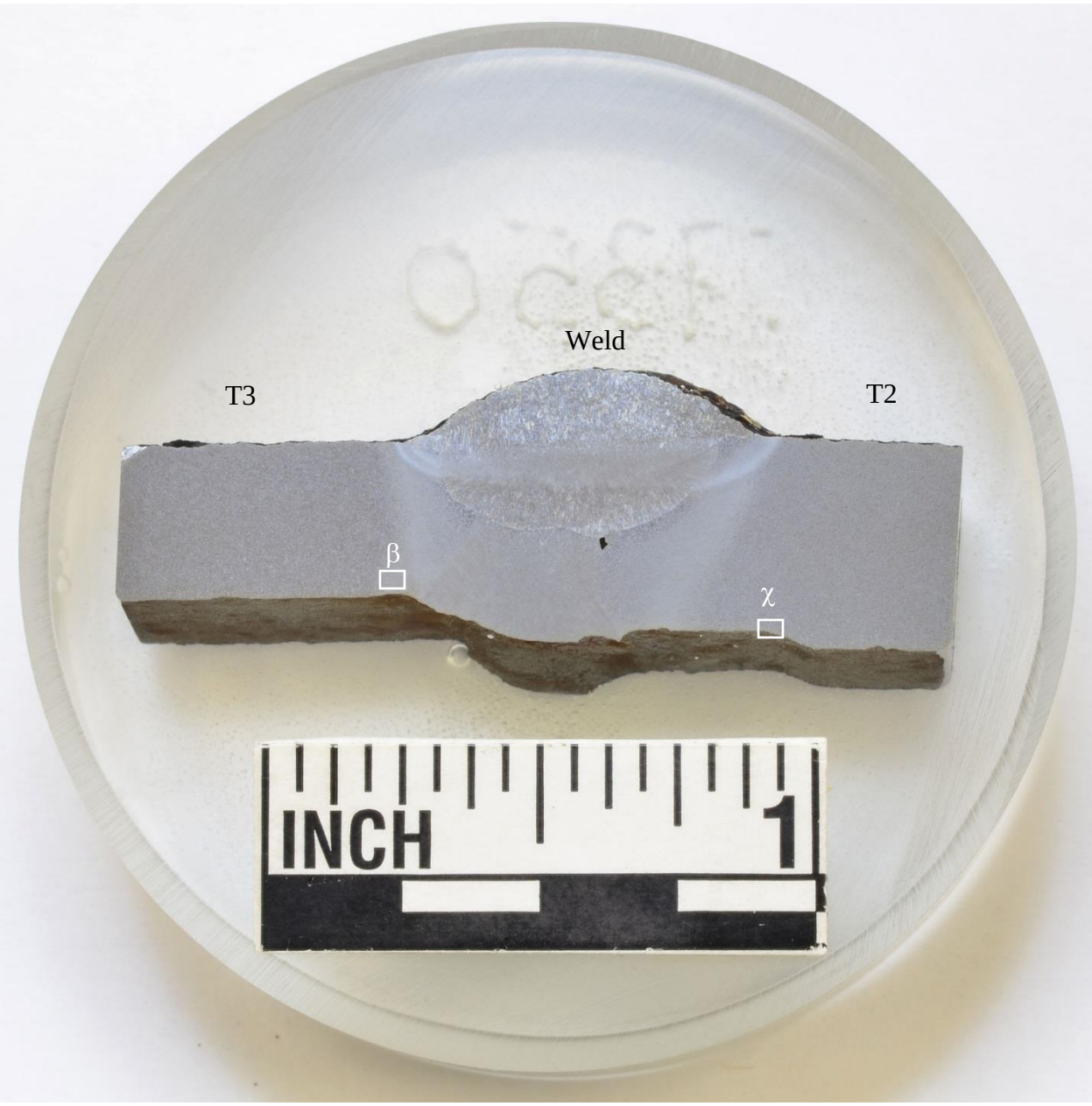

Figure 20 Photograph of the longitudinal section through the T2 to T3 weld prepared for metallography.

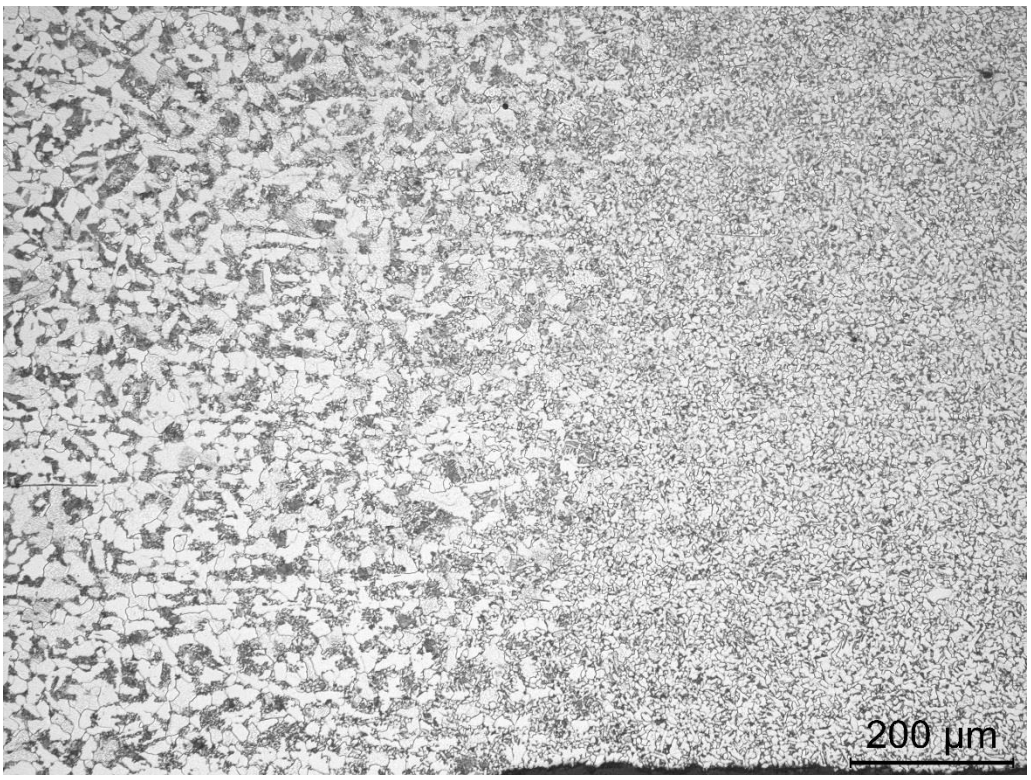

(a) 100X

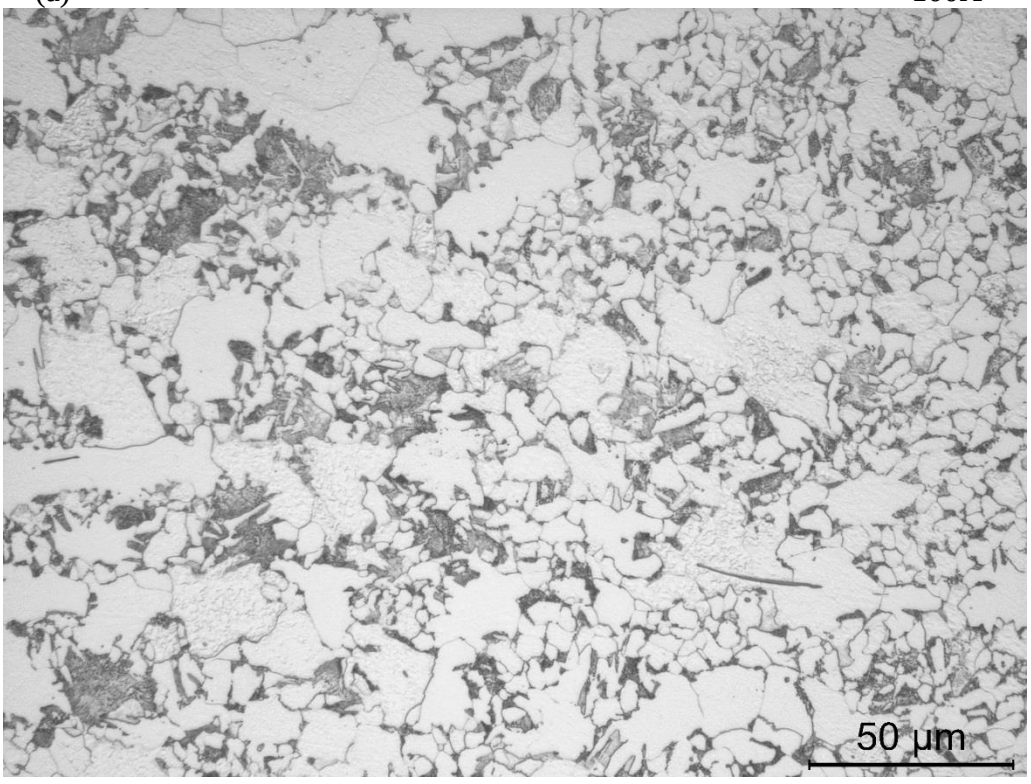

(b) 500X

Figure 21 Micrographs of the T3 weld heat affected zone, from the boxed region β Figure 20.

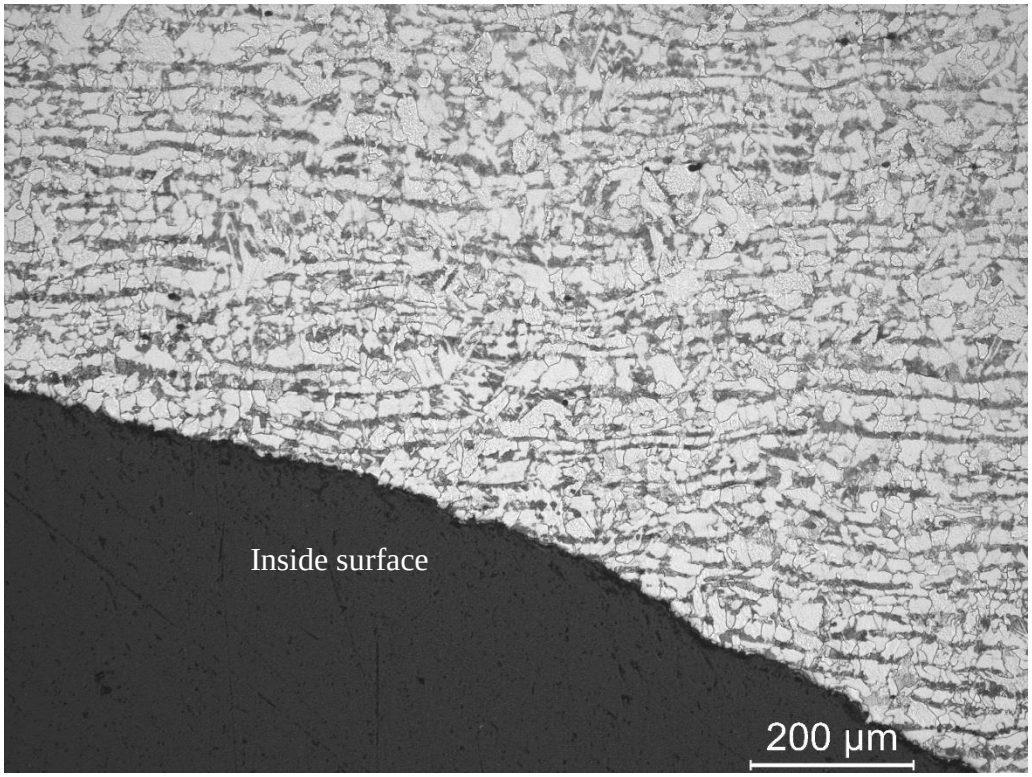

(a) 100X

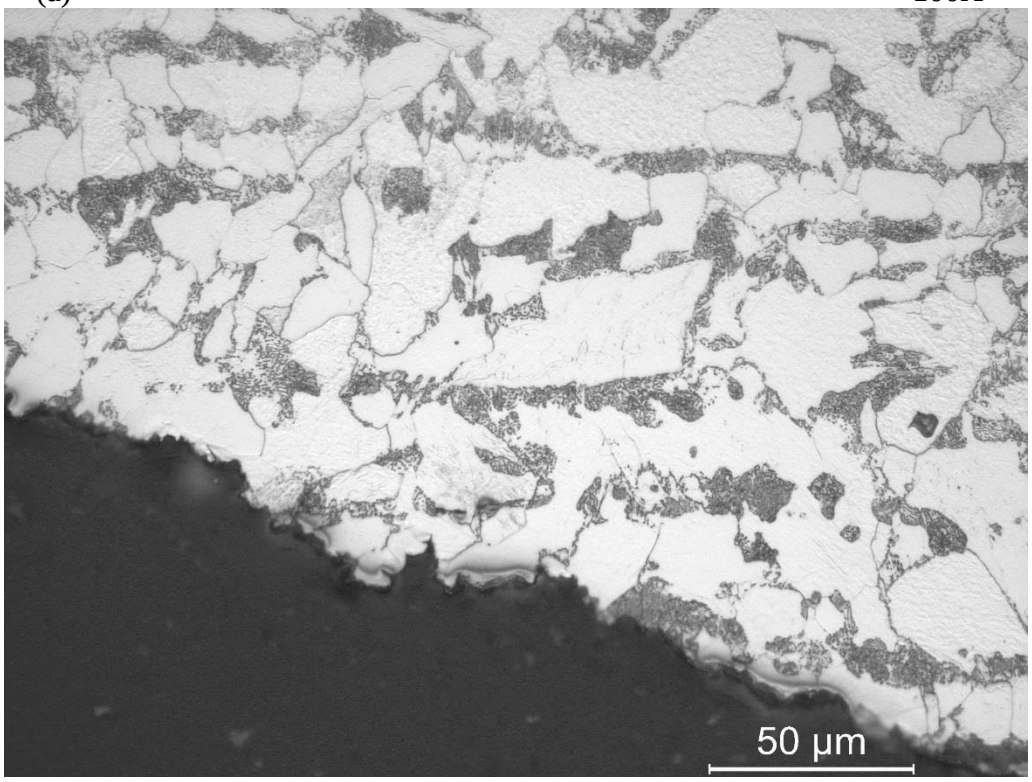

(b) 500X

Figure 22 Micrographs of the T2 weld heat affected zone, from the boxed region χ Figure 20.

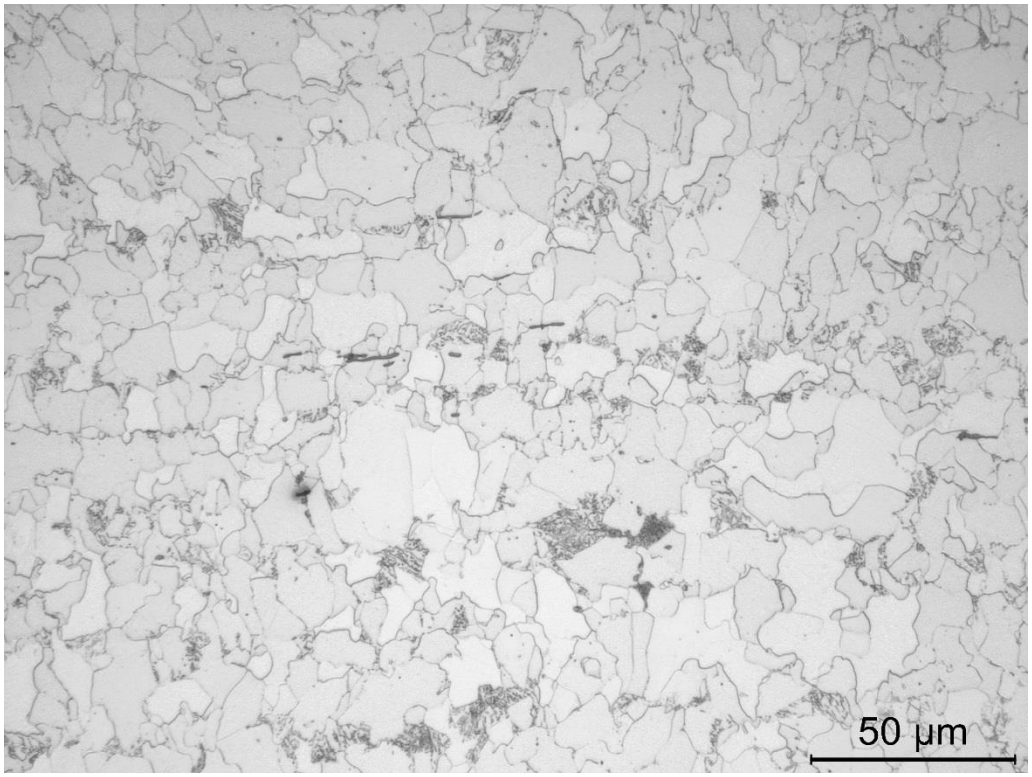

(a) Longitudinal 500X

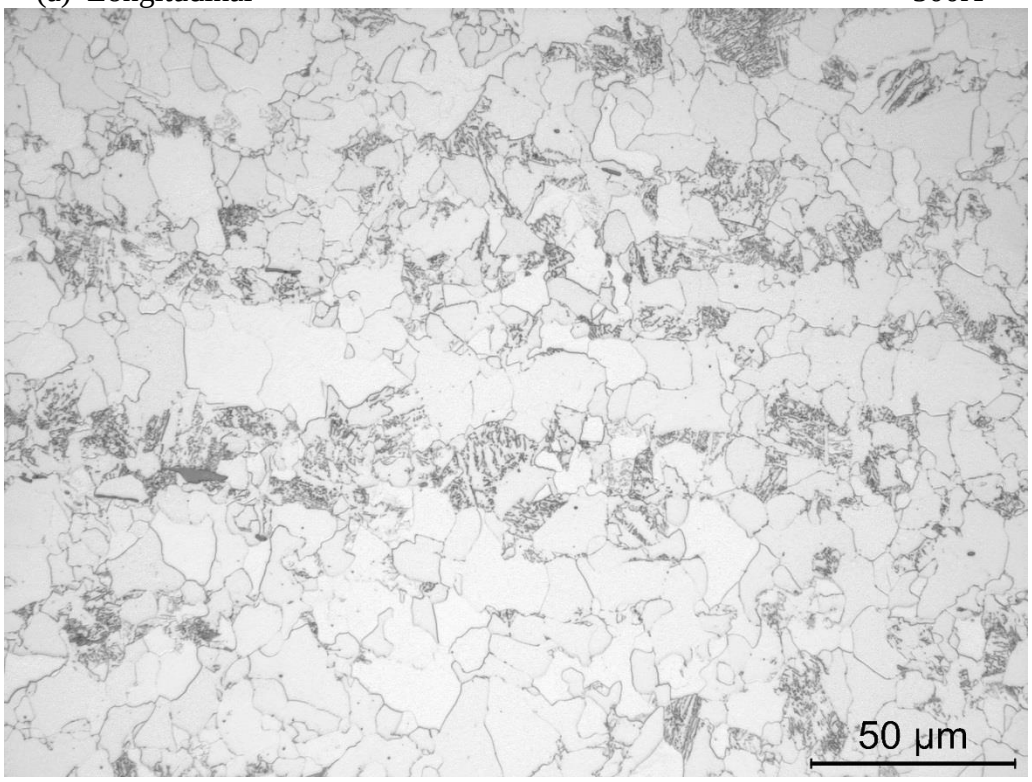

(b) Transverse 500X

Figure 23 Micrographs of longitudinal and transverse sections through elbow T1.

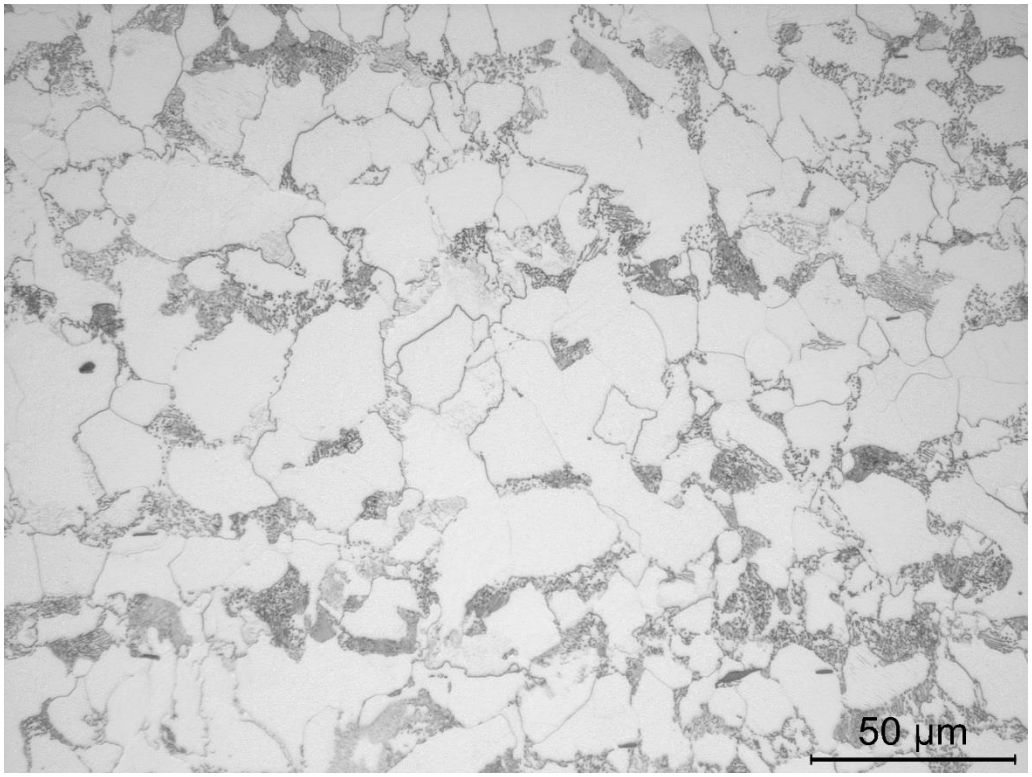

(a) Longitudinal 500X

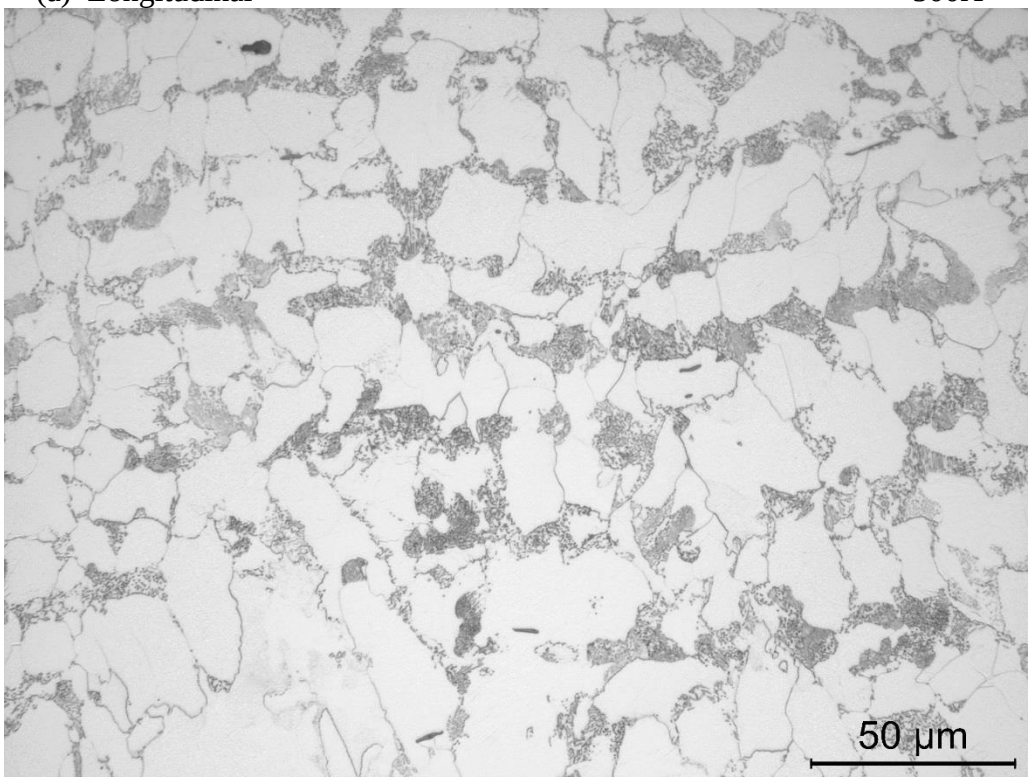

(b) Transverse 500X

Figure 24 Micrographs of longitudinal and transverse sections through elbow T2.

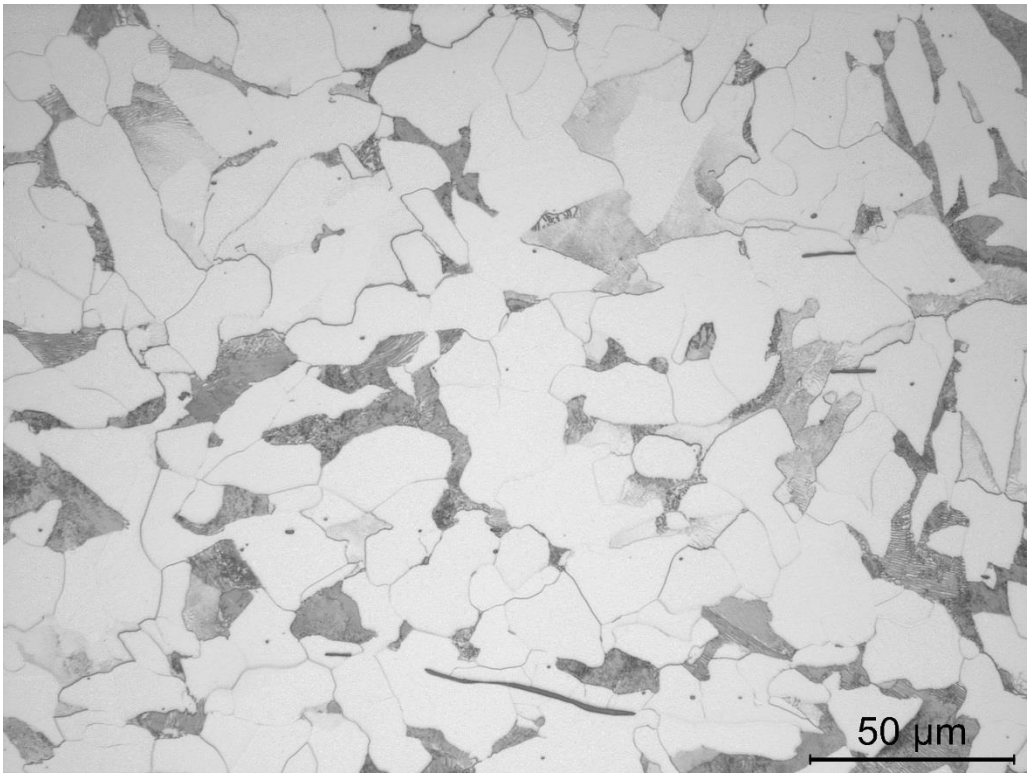

(a) Longitudinal 500X

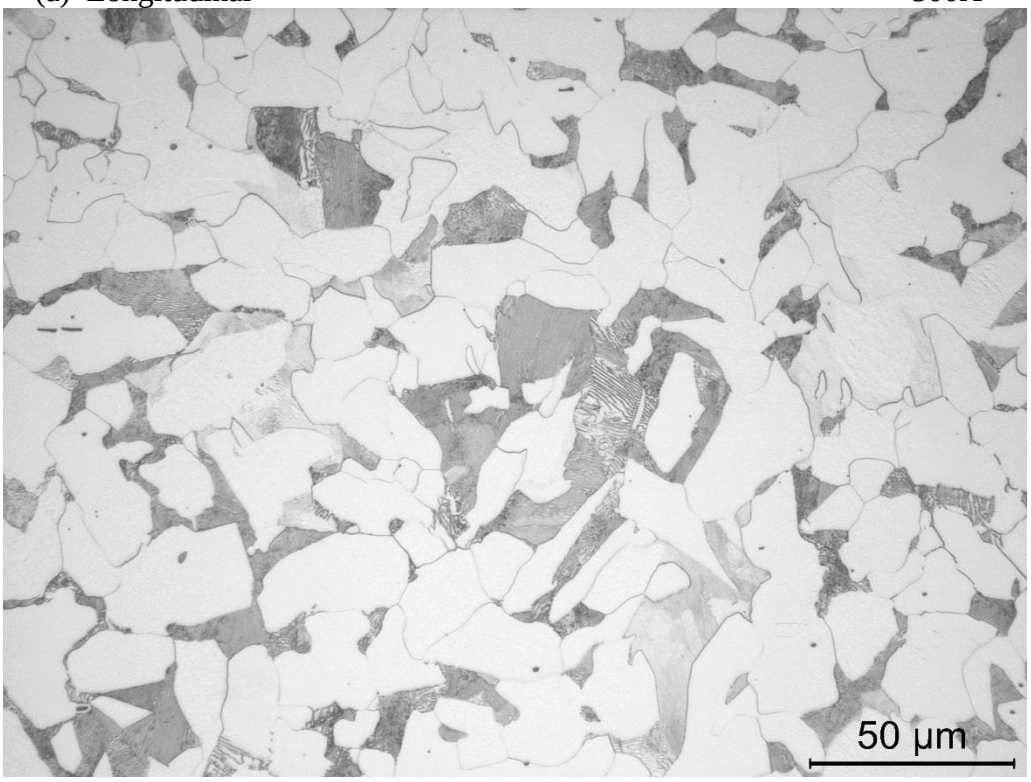

(b) Transverse 500X

Figure 14 Micrographs of longitudinal and transverse sections through pipe T3.

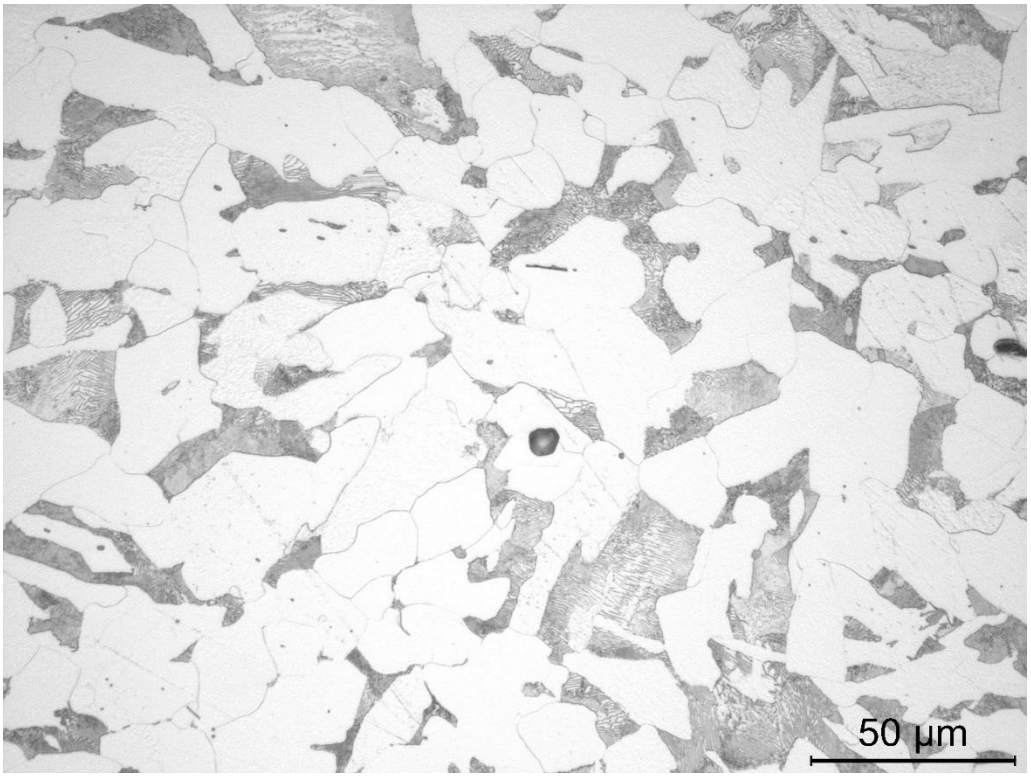

(a) 500X

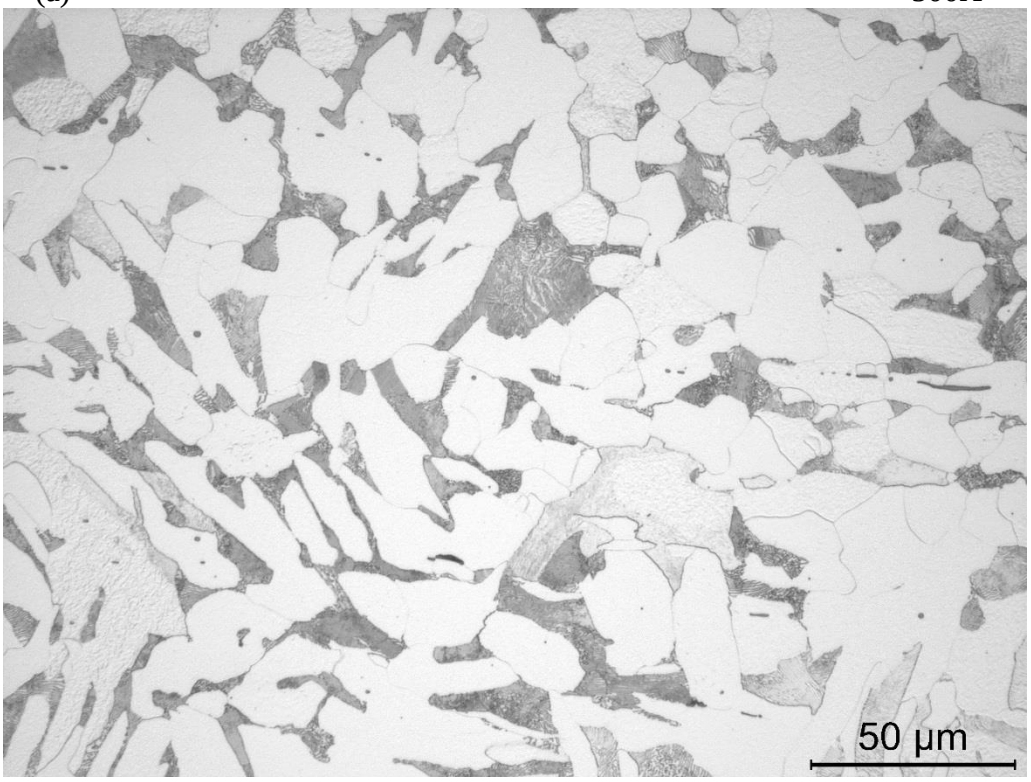

(b) 500X

Figure 25 Micrographs of longitudinal and transverse sections through pipe T4.